RADIO FREQUENCY ENERGY RECOVERY FOR PARTICLE ACCELERATORS

by

Veli Yıldız

B.S. in Physics, Boğaziçi University, 2008

Submitted to the Institute for Graduate Studies in
Science and Engineering in partial fulfillment of
the requirements for the degree of
Master of Science

Graduate Program in Physics

Boğaziçi University

2011

To the Memory of My Father

ACKNOWLEDGEMENTS

First of all, I want to thank to Professor Metin Arık for his supervision and guidance.

I want to thank to Dr. Roland Garoby and Dr. Fritz Caspers for letting me take part in RF Energy Recovery Project. I also want to thank to administration of Turkish Accelerator Center Project especially to the head of the project, Professor Ömer Yavaş, for giving me a chance to go to CERN and have this great experience.

I sincerely want to thank to Michael Betz for his guidance about electronics, all the work we have done together, for some of the figures in my thesis and for taking care of me when I got injured during my stay at CERN.

Son olarak, benden desteğini hiç esirgemeyen sevgili anneme sonzuz teşekkürlerimi sunuyorum.

ABSTRACT

RADIO FREQUENCY ENERGY RECOVERY FOR PARTICLE ACCELERATORS

During the operation of particle accelerators considerable amount of power coming to RF cavities is converted to heat in load resistors placed after RF cavities. When the CERN's Super Proton Synchrotron is analyzed as an example, it can be seen that 76 per cent of the power delivered to an RF cavity is dissipated in loads.

Under CERN-BE-RF-BR group, RF Energy Recovery Project had been started to study the feasibility of recovering this wasted power. This thesis mainly focuses on the work done during the feasibility studies in 2010.

Possible methods for recovering this wasted power was explained and feasibility was discussed. The method which is converting this excess RF power into DC power and utilizing was adopted. Overall recovery system and possible ways of converting RF power to DC power were discussed. For RF/DC conversion, resonant rectifiers which employ semiconductor diodes were chosen. Simulations were performed for different resonant rectifier architectures with PSpice. Most suitable circuit was chosen and prototype of this circuit was constructed. Measurements were performed for different input power levels, up to 400W, and RF to DC conversion efficiency reaching up to 88 per cent was reached.

ÖZET

PARÇACIK HIZLANDIRICILARI İÇİN RADYO FREKANSI ENERJİ GERİ KAZANIMI

Parçacık hızlandırıcılarının çalışması sırasında RF kovuklarına ulaşan enerjinin büyük bir kısmı yük dirençlerinde ısıya dönüştürülerek sistemden uzaklaştırılmaktadır. CERN' de bulunan SPS hızlandırıcısı bir örnek olarak incelendiğinde RF kaviteye ulaşan enerjinin yüzde 76' sının ısıya dönüstüğü görülebilir.

CERN'de boşa harcanan bu enerjinin geri kazanılabilirliğini araştırmak için CERN-BE-RF-BR gurubu altında RF Enerji Geri Kazanımı prjojesi başlatılmıştır. Bu tez proje gurubunun 2010 da yaptıgı çalışmaları özetlemektedir.

Boşa harcanan bu enerjiyi geri kazanmak için olası çözümler açıklanmış ve yapılabilirliği incelenmiştir. RF enerjisini doğru akıma dönüştürüp kullanma fikri benimsenmiştir. Sistem genel olarak açıklanmış ve RF doğru akım dönüşümü için olası yöntemler incelenmiştir. RF doğru akım dönüşümü için yarıiletken diyotlar kullanan rezonans doğrultucu devresi uygun görülmüştür. Farklı devreler için PSpice programı ile simülasyonlar yapılmıştır. Amaca yönelik en uygun devre seçilmiş ve prototipi üretilmştir. 400W' a kadar değişik güç değerleri için ölçümler yapılmış ve RF doğru akım dönüşümü için yüzde 88' e varan verim elde edilmiştir.

TABLE OF CONTENTS

LIST OF FIGURES

LIST OF TABLES

LIST OF SYMBOLS/ABBREVIATIONS

C_j	Junction capacitance
E_C	Conduction band energy level
E_F	Fermi level
E_V	Valence band energy level
I_{AC}	Alternating current
I_{DC}	Direct current
R_L	Load resistor
V	Voltage
α	Alpha (particle)
ϵ	Permittivity
Φ	Work function divided by electron charge
χ	Electron affinity divided by electron charge
Ω	Ohm
AC	Alternating Current
ADS	Accelerator Driven Systems
CERN	European Organization for Nuclear Research
CW	Continuous Wave
CWC	Cyclotron Wave Converter
DC	Direct Current
LHC	Large Hadron Collider
MATLAB	Matrix Laboratory (computer program)
NASA	National Aeronautics and Space Administration
PC	Personal Computer
PS	Proton Synchrotron
RF	Radio Frequency
SMA	Surface Mount Assembly
SMD	Surface Mount Device

SPICE	Simulation Program for Integrated Circuits Emphasis
SPL	Superconducting Proton Linac
SPS	Super Proton Synchrotron
VNA	Vector Network Analyzer

1. INTRODUCTION

1.1. High Energy Physics and Particle Accelerators

High energy physics or particle physics is a branch of physics which studies fundamental particles and the forces which act between them. The study of building blocs of matter has always been a great interest for all, in particular for physicists.

At the subatomic level, the structures under scrutiny are extraordinarily small, so visible light is inadequate in order to perform experiments at subatomic scale. For that reason some other techniques were needed to examine the atoms in detail. After the discovery of α particle, Ernest Rutherford carried out some experiments by bombarding different materials by natural α particles. In 1906 he bombarded mica sheet with α particles and observed the scattering of particles [1]. Then, in 1919 he bombarded nitrogen nuclei with α particles and induced a nuclear reaction. Because beams of α particles could be obtained with low intensity and fairly low kinetic energy, progress was limited. In addition to that, when heavier elements are bombarded with α particles, the strong repulsive force exerted on α particles by the heavy nuclei make it difficult for α particles to reach the nuclei.

Working with particles like proton or deuteron which have only one positive charge would be more effective than working with α particles. Because of having a single charge these particles would experience less repulsive force and get close enough to target nuclei. Protons or deuterons could be obtained but their energies were also low. Some device was needed to accelerate these particles to higher energies.

In 1928, encouraged by Rutherford, John. D. Cockcroft and Ernest T. S. Walton started designing an 800keV accelerator based on voltage division. With the first proton accelerator, in 1932, Cockcroft and Walton were able to split the lithium atom [2].

In 1924, Gustaf Ising, a Swedish physicist, proposed time varying electric fields across the drift tubes. In 1927, Norwegian engineering student Rolf Wideröe used Ising's principle and built a machine with alternating electric field with frequency of one megahertz [1]. He accelerated potassium ions to 50keV using only 25kV potential difference between two consequent drift tube electrodes. It was clear that with a sequence of more drift tube electrodes the particle beam could be accelerated to higher energies.

In 1929, Ernest Lawrence inspired by Wideröe and came up with the idea that if the particle beam was bent in a circle by a magnetic field, the same accelerating electrodes could be used many times rather than using long sequence of electrodes. Then, he started building a machine which is now called cyclotron. Lawrence's cyclotron was able to produce 1.25MeV protons in 1932. He also split the atom just a few weeks after Cockcroft and Walton [3].

Since then, with the help of developing technology, different kinds of accelerating structures and particle accelerators have been designed and built. These accelerators have given rise to new discoveries in the area of particle physics, letting people have more and more knowledge about fundamental particles and the forces which act between them.

1.2. RF Cavities

Until the late 1920s, the best method for accelerating charged particles was to let them pass through a gap with potential difference between two ends. By this method particles gain energy equal to voltage across the gap multiplied by their charge. However, energy gained by particles are limited because sparking occurs above a certain voltage.

In 1927, Rolf Wideröe developed another way of accelerating charged particles without the use of high voltage. His method was based on resonating particles with alternating electric field in order to give additional energy on each traversal of the field

between drift tubes (See Figure 1.1). However, Wideröe's linac was only efficient for low energy heavy ions because it requires very long drift tubes for high energies unless the frequency can be increased. Wideröe's linac was not practical at frequencies higher than 10MHz because the linac is actually the RF generator so that at high frequencies drift tube electrodes would start acting like an antenna and radiate power into free space which increases linearly with frequency.

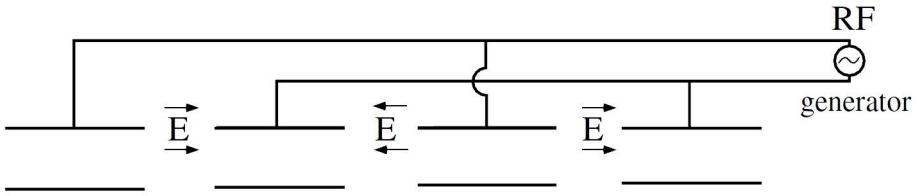

Figure 1.1. Wideröe Linac.

With the need of radars in World War II, the technology for high frequency power sources was developed. After the World War II, high power and high frequency RF sources became available. In 1948, Luis W. Alvarez developed Wideröe's idea and transformed Wideröe linac into RF cavity [4]. Alvarez structure encloses the accelerator in a conducting tank (See Figure 1.2). It is a resonant structure which is inductively coupled through a power coupler inserted through the wall of the resonant tank containing the drift tubes. Drift tubes shield the particles when the electric field is in the wrong direction. Rods connecting drift tubes to conducting tank are supporting the drift tubes. Unlike the Wideröe linac, the rods do not conduct RF current coming form the generator. The RF power for the cavity is delivered through the power coupler. The first Alvarez linac was operating at the frequency of 201.25 MHz and reached 32 MeV proton beam energy.

RF cavities can be classified according to different aspects. When the wave pattern inside the RF cavity is concerned there are two basic accelerating structures namely traveling wave cavity and standing wave cavity.

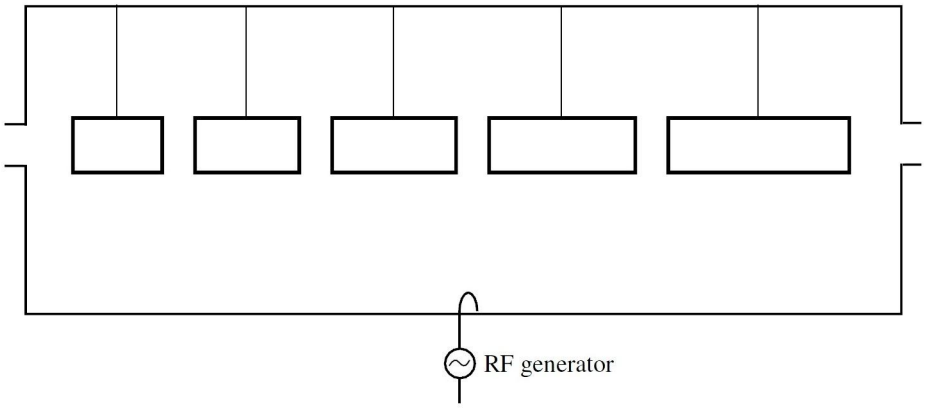

Figure 1.2. Alvarez Linac.

1.2.1. Standing Wave Cavity

RF cavity is a conducting tank. Solutions of Maxwell's equations in RF cavity with the boundary conditions on the conductor gives us the electromagnetic field configurations in the cavity. Different electromagnetic field configurations are called the resonant modes. One of these modes with electric field along the longitudinal direction on the axis is chosen for acceleration. The geometry of the cavity must be calculated so that the frequency of accelerating mode matches to the RF frequency. Desired mode in the RF cavity is excited through a power coupler which transfers electromagnetic energy into the cavity.

In standing wave structure there are two waves propagating in different directions resulting in standing wave pattern in RF cavity. Standing wave cavities are necessary for accelerating oppositely charged particles in opposite direction in the same accelerator.

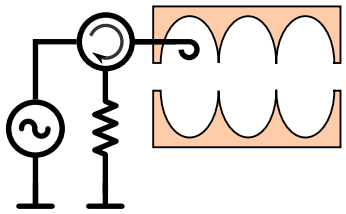

Figure 1.3. Feeding a standing wave cavity [5].

Figure 1.3 shows the scheme for RF structure of a standing wave cavity. RF power is transferred through wave guides or coaxial lines from RF generator to RF cavity. A power coupler connects transfer lines to cavity and excites the desired accelerating mode in the cavity. RF power should not reflect back to generator, so reflected RF power from the cavity is directed to load resistor by a circulator. Excess power that is reflected from the cavity is terminated in load resistor.

1.2.2. Traveling Wave Cavity

A traveling wave can be used to accelerate the particles in a cavity. In a cylindrical waveguide, waves propagate with phase velocities grater than the speed of light. Because particles can not travel at speeds faster than the speed of light, particle beam can not obtain any net acceleration. If the waveguide is loaded by some periodic obstacles the phase velocity of the wave can be slowed down to usable value. When the phase velocity is adjusted to the beam velocity, particles can surf along the wave and accelerate.

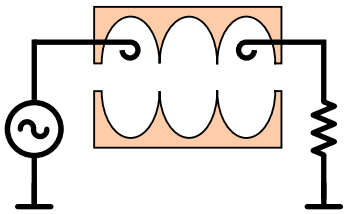

Figure 1.4. Feeding a traveling wave cavity [5].

A traveling wave structure is generally used to accelerate ultrarelativistic particles. These kind of cavities have two power ports at each ends of the cavity (See Figure 1.4). From one port RF power enters to the cavity and leave the cavity from the other one. The electric field travels through the cavity from the input port to the output port. In each port there are power couplers which connect transfer lines to the cavity. They play a role as matching unit between transfer lines and the cavity so that avoid reflection of RF power back to generator. After the cavity, excess RF power is sent to a matched load resistor and terminated.

1.3. CERN and Super Proton Synchrotron

The synchrotron is a particle accelerator, in which charged particle bunches follow a circular orbit and are accelerated to higher energies during circulation. Among circular accelerators, the synchrotron has the biggest size and, at present, it is the only one letting particles to be accelerated to energies at the order of TeV.

Two of the main parts of the synchrotron are magnets and RF cavities. Magnets are used for keeping the charged particles in a circular orbit and also focusing the particles in the beam pipe. The RF cavity is the part of the synchrotron where particles are accelerated in an electric field.

Today, Large Hadron Collider (LHC) is the World's largest particle accelerator. LHC was built by European Organization for Nuclear Research (CERN) to collide two counter rotating beams of protons or heavy ions. It is located near Geneva, where it spans the border between Switzerland and France about 100m underground. The LHC is not the only accelerator at CERN, it is the last and the largest ring in a whole chain of accelerators. Some of the other components of the chain are Linac2, Proton Synchrotron (PS) and Super Proton Synchrotron (SPS).

At the accelerator complex of CERN, protons are first accelerated by Linac2 and they are injected to PS Booster. The booster accelerates the proton beam to 1.4 GeV and then the beam is fed to the PS where it is accelerated to 25 GeV. Proton beam then sent to the SPS where particles accelerated to 450 GeV. After SPS they are finally sent to LHC both in a clockwise and anticlockwise direction.

The SPS is the second largest machine in CERN accelerator complex with a circumference of seven kilometers.

1.3.1. SPS Accelerating Structure

The SPS accelerating structure is based on high energy proton linacs with almost continuous wave (CW) operation. When SPS switched on in 1976, it was operating with two traveling wave cavities. In 1978 and 1979 another two cavities were added to SPS accelerating structure and started operating in 1980 [6].

Each SPS cavity consists of four sections with total length of about 16 m [7]. Each cavity is fed by a tetrode power amplifier which is located in a surface building above. Amplifiers are capable of delivering a CW output power of 500 kW at 200 MHz [8]. RF energy is transferred from amplifiers to cavities via a coaxial transmission line. They have characteristic impedance of 50Ω and air as dielectric material. Feeder lines can transport a traveling continuous wave of 750kW at 200MHz [8].

In order to operate with traveling wave structure, excess RF power at the end of the cavity must be terminated by matched load resistor (R_L) to avoid the reflection of electromagnetic wave at the end of the cavity. In figure 1.5, some components of RF structure of an SPS cavity can be seen. The part labeled as 1 is cavity tank with water cooling pipes attached around it. Above the cavity, with label 2, there are coaxial lines which carry RF energy from ground to SPS tunnel. RF loads which dissipate the excess power after the cavity is labeled as 3. RF loads have water as dielectric and they are capable of dissipating 500 kW of RF power [8].

In SPS cavities, a small part of the RF energy coming from amplifiers is transferred to beam or dissipated in cavity walls. However a big amount of power is converted to heat in load resistors.

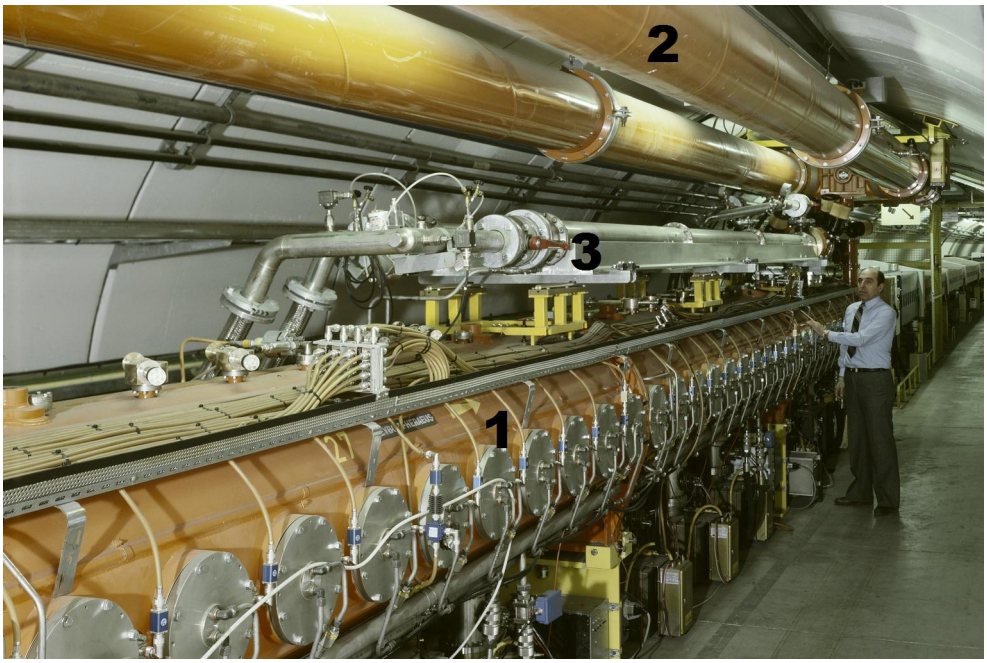

Figure 1.5. A view of an SPS cavity.

1.4. Need for RF Energy Recovery

1.4.1. An Example: SPS

In particle accelerators, different amounts of RF power is dissipated in RF loads to ensure the sustainability of the system. Calculating and comparing the amount of power which is supplied to an SPS cavity and the power dissipated in RF loads would help to realize how important RF energy recovery concept is.

Different acceleration cycles are used in SPS. During 2009 and 2010, the most used cycle was "Cycle 2009" [5]. This cycle repeats itself in every 42 seconds. Peak RF power per cavity for this cycle reaches up to 650 kW. Average output power of power amplifiers over one cycle can be taken as 254 kW [5].

Coaxial lines which deliver power from power amplifiers to RF cavities have some attenuation. Total attenuation between power amplifier and the cavity is 0.043 neper for a 110 m line [8]. It is approximately 0.347dB. Taking attenuation into consideration approximately 234kW RF power reaches to the cavity.

While the electromagnetic wave travels inside the cavity there is some energy dissipated in conducting cavity walls. Power dissipation per cavity is 13 kW [8].

Energy gain per cavity for one traversal is 1.27 MeV and average beam current is 70 mA citedome. Average potential difference that particles feel along the cavity is then 1.27 MV. Multiplying average potential difference that is felt by the particles along the cavity by average beam current gives us the power of 88.9 kW which is transferred to the beam when the beam is present in the cavity. During the mentioned acceleration cycle the beam is present for 47.4 per cent of the time. That gives us the average power of 42.1 kW which is transferred to the beam.

Amount of power reaching to a cavity is 234kW. 13 kW of this power is dissipated in cavity walls and 42.1 kW is transferred to beam. Excess power of 178.9 kW is dissipated in RF loads. This amount is 76 per cent of the power delivered to an RF cavity.

Not all accelerating structures waste that amount of power but when it is considered that SPS is just one of the components in CERN accelerator chain, wasted RF power will add up to a big amount for the whole chain. If RF recovery concept will be developed, CERN would save big amount of energy so that money. In addition to saving money, saving energy is also important for ecological issues.

1.4.2. Accelerator Driven Systems

Idea of using high intensity accelerators in nuclear energy development was proposed many decades ago [9]. Accelerator driven systems (ADS) have potential of transmutation of long lived radioactive waste as well as energy production.

In ADS protons coming from a high energy and high intensity accelerator produce spallation neutrons by hitting a heavy target. Spallation target is surrounded by a sub-critical core. Spallation neutrons produce nuclear chain reactions in the sub-critical core. In this way, nuclear fission energy is produced and the energy of input particles

is amplified [10].

The practical realization of ADS requires of a high energy (bigger than one GeV) and high current (bigger than 20mA) proton accelerator in order to produce spallation neutrons [11].

As far as the energy production is concerned, the efficiency of the system is important. If the value of effective multiplication factor of multiplying fuel in subcritical core is taken as k, the power gain, G, can be written as [9]:

$$G = G_0 \frac{k}{1-k} \tag{1.1}$$

Where G_0 is the ratio of average energy released in fission per emitted fission neutron (E_{fis}) and average energy cost of production of spallation neutron (E_n).

$$G_0 = \frac{E_{fis}}{E_n} \tag{1.2}$$

Average energetic cost of production of a spallation neutron is directly related to gain of the accelerator, G_{acc}. If we take the energy of a proton after whole acceleration process as E_{beam} and the average energy used for acceleration of a proton as E_p, we can write the gain of accelerator as:

$$G_{acc} = \frac{E_{beam}}{E_p} \tag{1.3}$$

If we take the number of spallation neutrons per an incident proton as n/p, we can write the average energy cost of production of a neutron as follows:

$$E_n = \frac{E_{beam}}{G_{acc}\frac{n}{p}} \tag{1.4}$$

Using Equation 1.2 and Equation 1.4 we can write G_0 as:

$$G_0 = \frac{E_{fis}}{E_{beam}} \frac{n}{p} G_{acc} \tag{1.5}$$

It was experimentally verified that for protons of energy one GeV and lead spallation target, the value of G_0 is about two [9]. However it is seen from Equation 1.3 that it can be increased with more efficient accelerators.

From Equation 1.1 and Equation 1.5 we can write overall gain of the system as follows:

$$G = \frac{k}{1-k} \frac{E_{fis}}{E_{beam}} \frac{n}{p} G_{acc} \tag{1.6}$$

As it is seen from Equation 1.6, gain of accelerator is directly proportional to overall gain of ADS. If the technology for RF recovery will be developed, it is obvious that ADS will be more feasible for energy production purposes.

2. DISCUSSION OF POSSIBLE SOLUTIONS FOR RECOVERING RF POWER

2.1. Feeding Cavity with Excess RF Power

First thing that comes to mind while considering RF energy recovery is that if we can redirect the excess RF power to cavity input or not. It is theoretically possible to feed the cavity with the excess RF power from cavity output (See Figure 2.1). While considering and examining this system, the most important thing is to ensure the sustainability and reliability of the accelerating system.

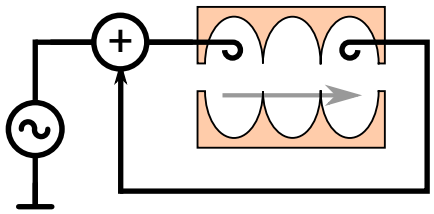

Figure 2.1. Schematic view of redirecting the excess power to cavity input [5].

Transport lines coming from power generator and coming from cavity output can be combined using a RF power combiner. The phase angle of the RF signal coming from cavity input can be adjusted to RF signal coming from generator so that constructive interference occurs [5].

However, as frequency and amplitude of output signal is concerned, cavity is not a time invariant system. For circular accelerators, as particles gain energy, RF frequency is adjusted so that particles and cavity stays synchronous. Amplitude of the RF signal coming from generator can also be varied for desired acceleration. Moreover, for the accelerators with injection energy lower than transition energy, RF phase must be changed very quickly when the transition energy is being crossed [12]. It would not be possible to change the phase of RF output of cavity, making it impossible to feed the cavity from its output during transition.

Beam loading,even for linear accelerators, constitutes the main problem for this approach. When particles pass through the cavity, they induce electromagnetic field inside the cavity and induced field disturbs RF amplitude. Passage of bunches will appear as pulses at the RF output of the cavity. In order to compensate, the signal coming from RF generator must be adjusted so that when signals form RF generator and from cavity output interfere we must get the desired RF amplitude. It is theoretically possible to predict the disturbance in the signal from cavity output and arrange the generator output to correct it, even before it happens. However, in practice it is difficult and has potential problems for the overall accelerating system. There must be an additional control loop around the cavity and RF generator making the overall system more and more complicated. In addition, accelerating system is very sensitive to disturbances in the RF signal and we need to have stable amplitude and phase.

2.2. Converting Excess RF Power into DC Power

Different frequency values are used for different accelerating cavities. Some of the frequencies that are used at CERN are shown in Table 2.1[1] . Excess RF power at these high frequencies can not be used directly. A good option, for utilizing it, can be converting the voltage and frequency into usable values and directing this power into electrical grid. The most feasible way of doing this is first converting this RF power into DC power, then converting DC power to AC power. After DC to AC conversion, AC power can be directed to electrical grid.

Table 2.1. Accelerating frequencies of some accelerators at CERN.

Accelerator	Frequency	Reference
Linac2	202 MHz	[13]
SPL	352 MHz and 704 MHz	[14], [15]
SPS	200 MHz	[8]
LHC	400 MHz	[16]

[1]SPL is still in design stage. The corresponding frequency values in table 2.1 were foreseen for the operation.

RF power can be converted into DC power with following devices.

2.2.1. Cyclotron Wave Converter

Cyclotron wave converter (CWC) is a device that employs fast cyclotron wave of the electron beam to convert microwave power to DC power. CWC was patented in 2003 [17]. The CWC consists of an electron gun, a microwave cavity, a transition space aligned on the z-axis and a collector (See Figure 2.2).

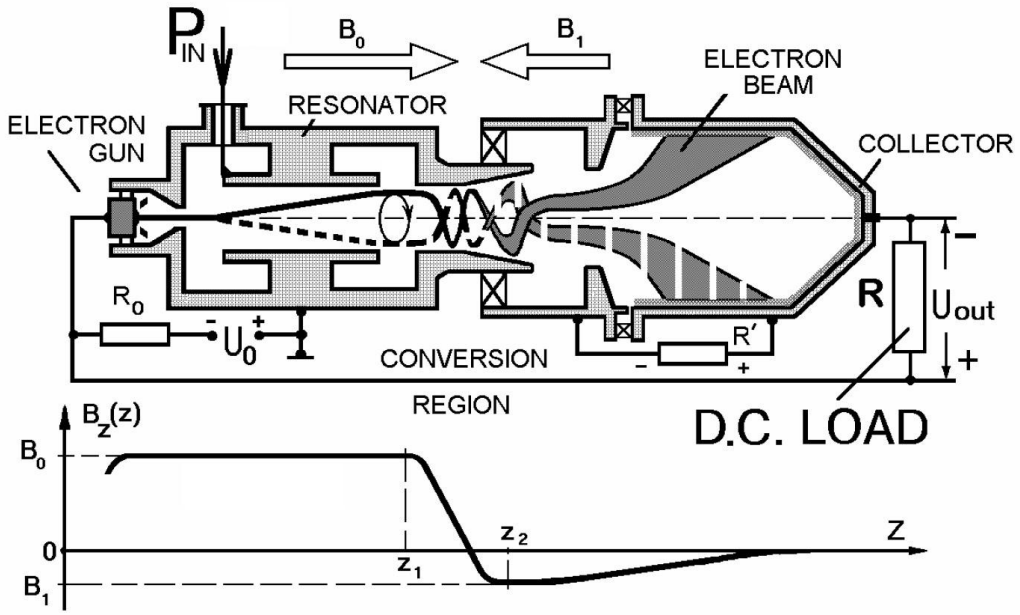

Figure 2.2. CWC [18].

The microwave cavity is subjected to a static and uniform magnetic field B_0 in the direction of z. The microwave cavity includes a resonator and a gap of interaction between the electrodes of resonator. The transition gap is subjected to another external static magnetic field B_1 in the direction of -z. Magnetic field is created by an external static magnetic field generator.

When the microwave cavity is subjected to a microwave power P_{IN} with frequency f_{MW}, resonator receives the P_{IN} and electrodes of the resonator create a transverse electric field alternating at the frequency of f_{MW} in the interaction gap. Therefore, the electron beam which is formed by the electron gun and injected in to the interaction region of microwave cavity, receives transverse kicks. With the effect of static magnetic

field B_0, electron beam obtains cyclotron rotation at frequency f_c. In the case of two electrodes the cyclotron frequency f_c is equal to microwave frequency f_{MW}.

In the transition region (z_1<z<z_2 in Figure 2.2) the cyclotron movement of the electron beam is converted into an axial movement. Because of the radial component of the static magnetic field, rotating electron beam receives additional Lorentz forces causing the z component of the velocity of the electron beam increase. Tangential component of the velocity of the electron beam decreases due to reversed magnetic field.

After the transition region accelerated electron beam enters the collector. At the collector the kinetic energy of the electron beam is extracted as a DC power in DC load resistor.

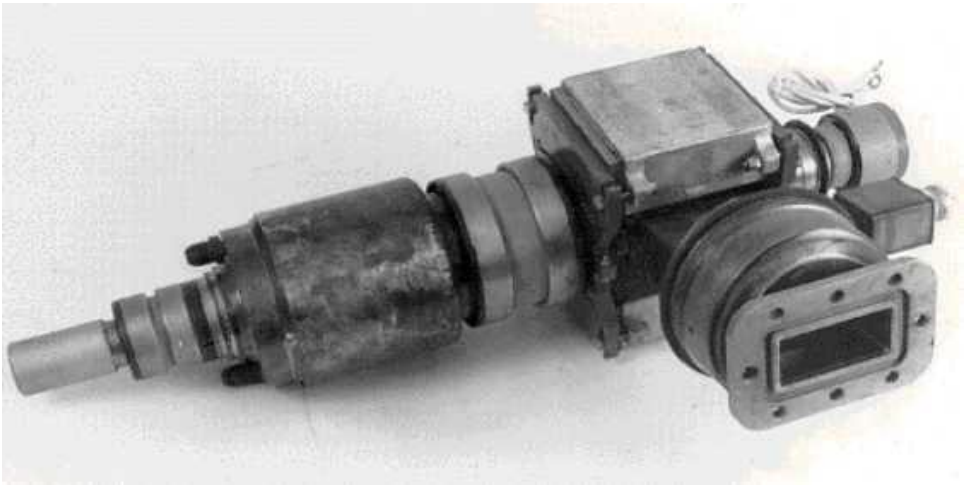

Figure 2.3. High power CWC of Tory Research and Product Corp [18].

Several high power CWC devices had been produced and tested by Troy Research and Product Corp. in collaboration with Moscow State University. A version of CWC developed by Troy Research and Product Corp. can be seen in figure 2.3. The efficiency between 60 and 70 per cent had been demonstrated at microwave power level of 10kW with the output DC voltage between 10kV and 20kV [18].

Some properties of CWC are given in table 2.2. As seen in the table, CWC would be useful in a frequency range between one GHz and 10 GHz. Power handling capacity

Table 2.2. Some properties of CWC [18].

Property	Value
Output power range	0.5 kW - 50 kW
Efficiency (demonstrated)	Up to 83 per cent
Frequency range	1 GHz - 10 GHz
Output voltage range	1 kV - 50 kV
Focusing system	Permanent magnets

of one CWC device may not be enough for RF recovery system, so it may be needed to use several devices. In this case, excess RF power after cavity can be divided and sent to several CWC devices in order to convert it into DC. DC output of each device can be combined afterwards and DC power can be sent to DC/AC unit.

2.2.2. Rectifiers

A rectifier is a device that allows current flow through it in one direction but not in the other. It is therefore an effective unidirectional conductor and is used mostly for converting alternating current to direct current.

Rectifiers have been used in the field of power transmission by radio waves since 1960s [19]. Power transmission can be defined as three stage process. At the first stage DC electrical power is converted into RF power, at the middle stage RF power is transmitted through space to some distant point and at the final stage power is collected and converted back to DC power. In order to have an effective energy transmission by this method, all three stages need to be efficient.

The first terrestrial application of wireless power transmission which was studied and experimentally examined was the microwave powered helicopter [20]. William C. Brown and his group constructed a microwave powered helicopter and made the first presentation in May 1963 [19]. It was in Raytheon's Spencer Laboratory where 400 W of CW power was transmitted through air and 100 W of DC power was retrieved and used to drive a DC motor.

While studying wireless power transmission one missing technology had been the conversion of microwaves directly into DC power to derive the motor. Because there were no satisfactory microwave rectifiers at that time, the U.S. Air Force funded some studies [19]. One of these studies was the investigation of semiconductor diode as an efficient rectifier and was carried out at Purdue University. After then, different types of diodes and different rectifier circuits are developed and examined to increase the efficiency and power handling capacity of rectifiers.

Later, in 1975, another demonstration of microwave power transmission was made by NASA at Goldstone Facility. Microwave power was transmitted between two points that are one mile far away from each other. The ratio of DC output power to incident microwave power was 0.84 [19] and over 30 kW of DC power was obtained.

During both studies (microwave powered helicopter and Goldstone demonstration of NASA), a device called rectenna was used in order to receive microwave power and convert it into DC power [19]. The term rectenna is actually combination of the words rectifier and antenna. Basically, rectenna consists of an antenna for receiving electromagnetic wave and a rectifier for converting microwave power to DC power (See Figure 2.4).

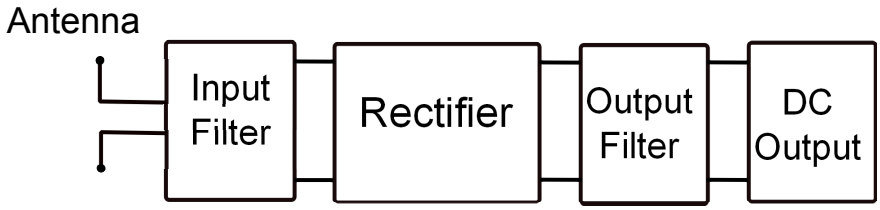

Figure 2.4. Components of a rectenna.

Frequency range of CWC does not include frequencies lower than one GHz (See table 2.2). Rectifiers can be used for recovering RF power from accelerators which operate at low frequencies. Power handling capability of a single rectifier device is comparably low. Several rectifying units must be used for RF recovery. RF power is needed to be coupled with antennas after RF cavity and sent to rectifying units. After conversion of RF power into DC power in rectifying units, DC power can be combined. Then DC power can be sent to DC/AC unit.

3. OVERVIEW OF RF ENERGY RECOVERY

Starting from here, this thesis will focus on the feasibility research for RF energy recovery which was held in 2010 at CERN for SPS accelerating cavities.

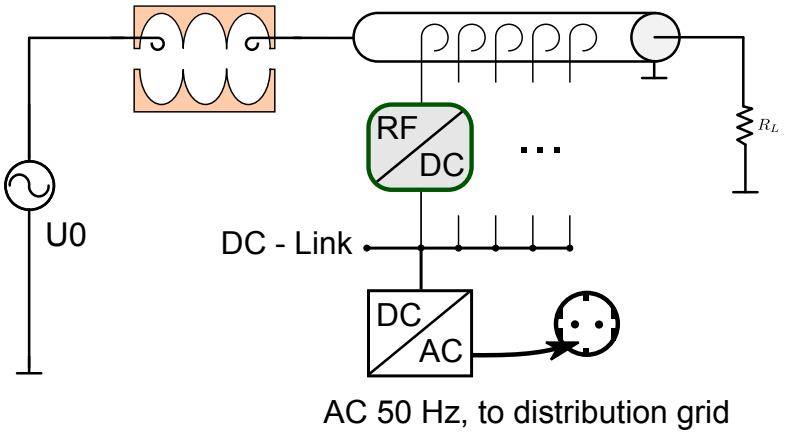

Figure 3.1. Overview of RF energy recovery system [5].

A foreseen overview of RF energy recovery concept is shown in Figure 3.1. Overall system mainly consists of a power divider, RF/DC unit and DC/AC unit.

As seen in Figure 3.1, coaxial line after RF cavity is replaced by a power divider. Power divider will couple RF power and 50Ω coaxial cables will carry this power to RF/DC modules. DC output of RF/DC modules will be combined and directed to DC/AC unit. After conversion of DC to AC, power can be used for feeding the electrical grid.

Overall system must be matched so that it does not constitute a possible problem for the accelerating structure. It must be safe and reliable that in the case of failure of any component, there must not be any reflected power back to RF cavity.

3.1. Power Divider

In the current status of SPS RF cavities, the excess power is carried away with coaxial lines, placed after RF cavities. In Section 1.4.1, it was shown that during

mentioned acceleration cycle average excess power of 178.9 kW is dissipated in RF loads. However coaxial lines may have peak input power of 500kW [21]. With the current technology, this amount of power is impossible to convert into DC power with a single semiconductor device. Therefore the excess RF power must be split into multiple units. This is to be done with a power divider placed after RF cavity. The power divider is based on a coaxial line with characteristic impedance of 50Ω and it has air as dielectric material. Diameter of its inner conductor is 100mm.

Coupling units will be placed inside the coaxial line to couple the RF power in order to deliver it to RF/DC modules. Power level of one kW was chosen for the RF/DC modules. Therefore, with the coupling units constant power of one kW must be coupled and send to RF/DC modules. Different solutions were analyzed for coupling units.

- Electrical coupling with a pin.
- Electrical coupling using a pin with a capacitive plate at the end to increase the coupling.
- Magnetic coupling using a loop.

Electrical coupling with a pin is too week for the application. Last two options give similar levels of coupling for the same dimensions. However, materializing electrical coupling using a pin with a capacitive plate is much easier than materializing magnetic coupling using a loop [21]. So that, the best solution for the coupling is using antennas consisting of a pin and a capacitive plate attached to its end. The power along the divider is decreasing linearly after each coupling unit. In order to keep the power delivered to RF/DC modules constant at one kilowatt level, coupling must increase for each unit along the divider. This can be realized by varying the height of the pin and the length of the plate. Because of the low RF power at the end of the divider, dimensions of coupling antennas need to be too big. For this reason, it is convenient to couple power until it drops to 50kW in divider and let 50kW power dissipate at R_L. Allowing 50kW power being absorbed by R_L results in 90 per cent of divider efficiency.

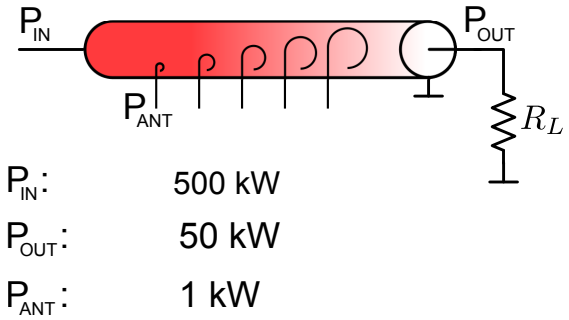

Figure 3.2. Power divider [5].

It was planned that the divider will couple RF power at 45 stages. Each stage has 10 coupling antennas distributed around the inner surface of the outer conductor of the coaxial line (See Figure 3.2). The overall length of the divider is about five meters [21]. After coupling antennas, coupled RF power will be delivered to RF/DC modules by coaxial cables with characteristic impedance of 50Ω

3.2. RF/DC Modules

Foreseen overview of RF/DC module is shown in Figure 3.3. Power level of one kW was chosen for an RF/DC module (See Section 3.1). RF power will pass through a circulator and reach a power splitter. Splitter will divide power into four and send 250 W power to each rectifier. RF power will be converted into DC power in rectifier.

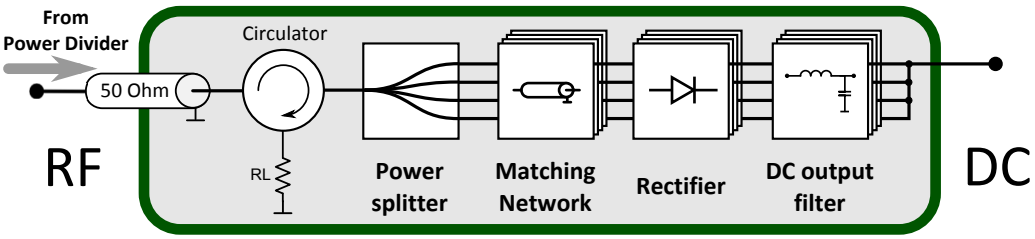

Figure 3.3. Overview of RF/DC module [5].

Semiconductor diodes are used in rectifying units. Temperature changes affect operation of diodes. In order to keep the components safe and ensure the reliability of the system, RF/DC module must be cooled. Water cooling system is available in SPS tunnel so RF/DC module can be water cooled.

3.2.1. Circulator

RF/DC module must be isolated from power divider in order to avoid any reflected power reaching back to divider. In the case of a failure at RF/DC module, power coming from the divider must be terminated at load resistor. This can be achieved by a circulator.

A circulator is a device which passes power input from one port to the next one in a rotational fashion. It can be arranged to transfer the power from one port to the next one in clockwise or counterclockwise direction. Circulator is a non-reciprocal device that it only passes power in one rotational direction but not in the other.

In Figure 3.3, there is a circulator which passes power in clockwise direction. RF power is transferred from power divider with 50Ω cables to the circulator. Power enters from input port of circulator and transferred, in the direction of arrow, to the power splitter. If there occurs a problem in rectifiers the reflected power will be transferred to load resistor which is connected to third port of circulator. Because circulator is non-reciprocal device, there will be no power going back to divider from power splitter. Load resistor must be matched so that all the power that is delivered to the resistor will be terminated so that there will be no power going back to input port of the circulator.

3.2.2. Power Splitter

A single semiconductor device can not handle power level of one kW. One kW power that is coming from power divider can be split into four and power of 250 W can be sent to each rectifier. Using 250 W power level for the rectifying units will allow the system to be on the safe side. Splitting RF power coming from divider can be done with a four-way power splitter (See Figure 3.4). Another solution would be using three two-way splitters [5]. With first splitter one kW power can be split into two ports with 500 W. Then, using other two splitters after the first one, power can be split into four ports with 250 W.

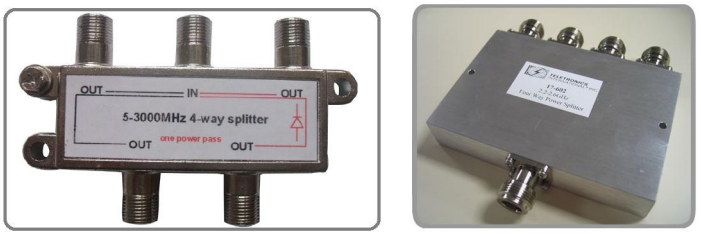

Figure 3.4. Four-way power splitters.

3.2.3. Matching Network

In order to have maximum power transfer to rectifier, impedance of rectifier must be matched to characteristic impedance of cable which delivers the RF power. Matching network provides a transformation of impedance, seen by rectifier, to a desired value to maximize the power transfer.

3.2.4. Rectifier

When rectifier and CWC are compared, it can be seen that CWC device have more power handling capacity. However, CWC operates frequencies higher than one GHz. For SPS operating frequency, 200 MHz, rectifiers seem to be the best option to employ for RF/DC units. However, a single rectifier can not handle amount of power coming from power divider, so multiple rectifying units must be used for an RF/DC module. Designed rectifier will be studied in detail in Section 5.3.

3.2.5. DC Output Filter

After conversion of RF power to DC power in rectifiers, DC output filter provides a clean DC at the output.

3.3. Combining DC Power and DC/AC Conversion

In order to redirect the recovered power to electrical grid, after conversion of RF power to DC power in RF/DC modules, output of each RF/DC module must be

combined. Then, power that is combined in DC link would be directed to a DC/AC inverter and be converted to AC power.

While using this system, one must ensure that failure of one or more RF/DC modules should not affect the overall system. Moreover, as it is shown in Section 5.2, rectifiers have a load resistor that is to use as a DC battery. For a maximum efficiency of RF/DC conversion, this load resistor has different values for different input RF power. DC load can be removed and output of all RF/DC modules can be combined using parallel and series combinations in order to reach desired voltage and current value [22]. Each rectifying unit must see the optimum output resistance value, which is changing with the input RF power, at its output to have maximum conversion efficiency of RF to DC. System must be able to track the optimum resistance value and adjust itself for maximum power efficiency.

Solar power systems use same kind of operation [23]. Solar power systems use photovoltaic cells to convert solar power to DC power. Number of photovoltaic panels in series form a string and a number of strings in parallel form an array. DC power of each array is combined and sent to inverter. While operating, one of the major tasks is to ensure that the photovoltaic module is operated at the maximum power point. In order to extract the maximum amount energy, the photovoltaic system must be capable of tracking the solar array's maximum power point which varies with the solar radiation and temperature. Studies have been done for tracking the maximum power point for photovoltaic systems(For details see references [23], [24] and [25]).

DC/AC inverters for solar power systems for different power levels are available in the market. Some of the power levels of available inverters are 250 kW, 375 kW, 500 kW and one MW.

4. SEMICONDUCTORS AND DIODES

Rectifier circuits employ diodes for allowing current flow through it in one direction but not in the other. Circuit components generally include parasitic electrical parameters. Parasitic parameters of diodes produce undesirable effects at high frequencies. In this chapter, principles of semiconductors as well as p-n junction diodes and Schottky diodes will be explained. P-n junction diodes and Schottky diodes will be compared. AC equivalent circuits of diodes will be given and causes of parasitics will be explained.

4.1. Semiconductors

A single atom has energy levels which can be occupied by electrons. In the case of a solid crystal, the atomic nuclei are very close together so the electrons in one atom are influenced by the neighboring atoms [26]. As the atoms come close together, the energy levels of the electrons broaden into bands of allowed values. Energy bands which electrons can not occupy are called forbidden bands.

Solids comprising metals consists of atoms close to each other, so their electrons occupy bands of energy. In metals, the outermost electrons of the atoms occupy valence band. Valence band is partially filled with electrons and adjacent higher levels are unoccupied. When metals are connected to a battery, valence electrons gain energy and they can move to higher unoccupied energy levels which fall into conduction band. These electrons are carriers of current in metals.

In the case of an insulator the valence band is completely filled by electrons. The energy level between conduction band and valence band, forbidden band, is so wide, for that reason electrons can not gain sufficient energy when an insulator is connected to a battery. Thus no carriers are available for conduction.

Semiconductors are solids which have electrical properties between those of conductors and insulators. The separation between the energy of lowest conduction band and that of the highest valence band is called band gap. Semiconductors have a band diagram similar to that of insulators but energy gap between valence band and conduction band is narrow. A simplified band picture of solids is given in Figure 4.1.

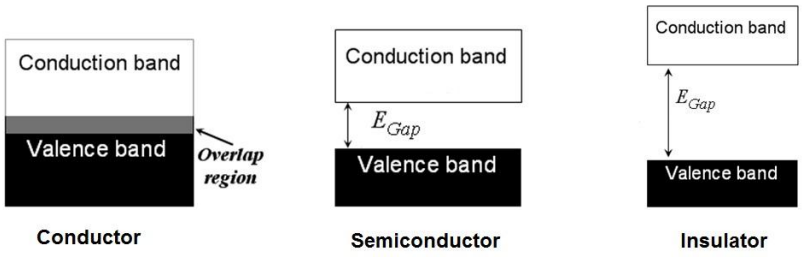

Figure 4.1. Schematic view of band structure of solids.

4.1.1. Electric Current in Semiconductors

At zero Kelvin, a pure semiconductor is an insulator. However as the temperature of the semiconductor rises above absolute zero, an electron which is loosely bounded in valence band can gain sufficient thermal energy to reach the conduction band and become a free electron. When electrons leave the valence band and move to conduction band, holes are left in the valence band. Holes are simply unoccupied states in the valence band. Other electrons in valence band can then move from their atoms to fill these unoccupied states, leaving a hole in the energy level they came from. This movement results in the movement of holes in the crystal.

Valence band electrons can not carry any current. However, holes move in the opposite direction of that of electrons so it can be considered as the movement of positive charge equal to charge of an electron. When there is no electric field, the movement of holes are completely random and the number of holes are equal to number or free electrons. When an electric field is applied to a semiconductor electrons drift in one direction so that holes act like positive charges and drift in the opposite direction. While conduction of current is achieved by only by electrons in a metal, the current through the semiconductor is carried, in the same direction, by conduction electrons

and by holes.

4.1.2. P-type and N-type Semiconductors

Addition of impurities to a semiconductor is called doping. Doping a semiconductor material changes its electrical properties. For example when a tiny amount of pentavalent element, donor, added to silicon, four valence electrons of donor material form covalent bonds with the surrounding silicon atoms while the fifth electron is bond loosely to donor atom. Ionization energy of the atom is at the same order of thermal energy of the electron at ordinary temperatures. Thus, donor atoms are ionized and leave a free electron into the crystal. This type of semiconductor, which has excess electrons, is called n-type semiconductor. Electrons are majority carriers in n-type semiconductors and holes are minority carriers.

When atoms with three valence electrons are added into silicon, bonds are formed between the material added, acceptor, and silicon. However because acceptor material has only three valence electrons, an additional electron can move from silicon to acceptor atom to form four covalent bonds leaving a hole in the silicon atom. This type of semiconductor is called p-type semiconductor. Holes are majority carriers and electrons are minority carriers in p-type semiconductors.

4.2. P-n Junction Diodes

As explained above, electrical properties of a semiconductor is altered by doping. However that does not give us a useful device. If p-type and n-type semiconductor are let defuse into each other, as in Figure 4.2, holes in p-type diffuse into n-type semiconductor and electrons in n-type diffuse into p-type semiconductor. Diffusion causes collection of excess electrons at one side of p-n junction and collection of excess holes in the other side, resulting a potential difference, V_j, between two sides of p-n junction (See Figure 4.2). V_j is called diffusion potential difference or junction barrier [26]. There occurs an electric field between two sides of the p-n junction and any electrons or holes in this region is swept away by this field [27]. This way p-n junction

is depleted of charges so it is also called depletion region.

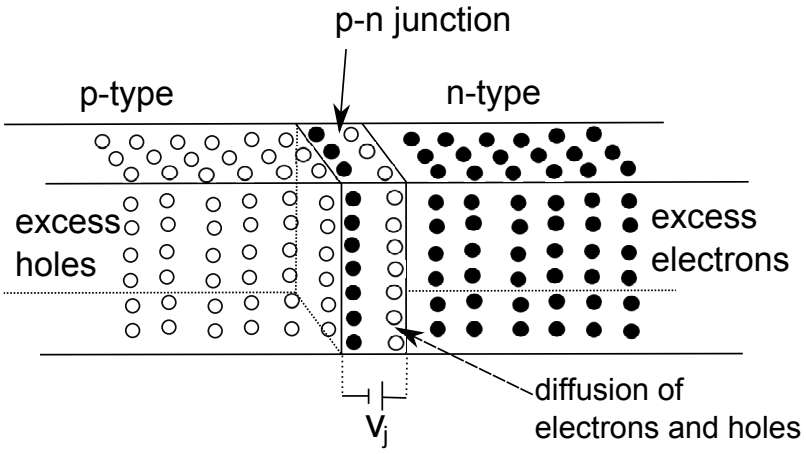

Figure 4.2. P-n junction [26].

When a battery is connected across the p-n junction diode with its positive pole to p-type semiconductor and negative pole to n-type semiconductor, the diode is said to be forward biased (See Figure 4.3). If applied potential difference is greater than junction barrier than more holes urge from p type material to n type material and more electrons urge from n type to p type material[26]. Current, resulting from the movement of holes and electrons, starts flowing across the junction. As seen in Figure 4.3, when the potential across the diode is increased the current increases exponentially.

If the poles of the battery are exchanged and its positive pole is connected to n-type material and negative pole is connected to p-type material, then the diode is reverse biased. Now the applied potential and junction barrier has the same polarity so that the applied potential adds to junction barrier and increases the electric field across the junction. No majority carriers can drift across the junction. Instead, holes, which are minority carriers, from n side urge to p side and some of the valence electrons in p fills the holes increasing the positive charge density at p side. Similarly, electrons drift from p side to n side and increase negative charge density in n side. As it is seen, in the case of reverse bias movement of minority carriers cause a current which reaches a small maximum value as potential difference is increased. This current, which occurs when the diode is reverse biased, is called leakage current and it harms operation of diode at high frequencies.

As discussed above, current flow through the p-n junction diodes has some interesting behavior. This behavior is not governed by Ohm's law so the diode has a nonlinear and also rectifying behavior.

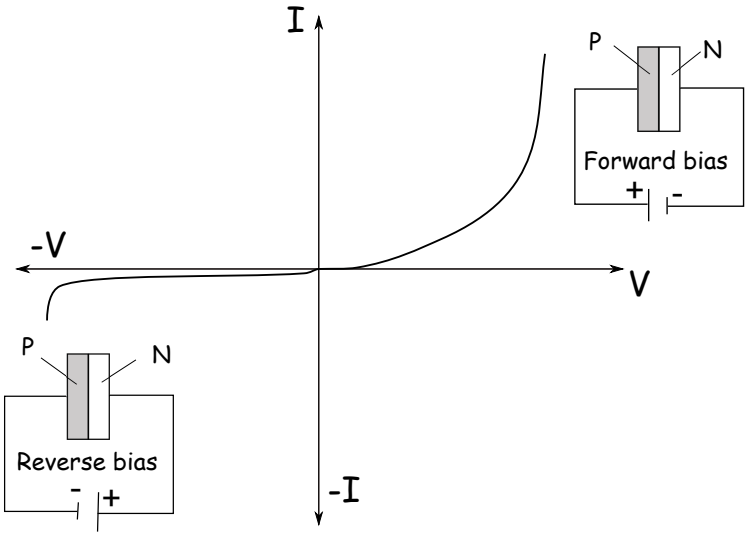

Figure 4.3. Voltage current characteristics of a junction diode [26].

4.3. Semiconductor Junctions With Metals

Metals are essential for electronic devices. In order to connect the diodes to circuit, metals are necessary. Under proper conditions, they are also able to produce rectifying junctions that can be used to control the response of semiconductors. Schottky diodes have metal-semiconductor junction and characteristics similar to that of p-n diodes except that for many application they have much faster response.

Figure 4.4 shows some important energy levels in metals and n-type semiconductors with respect to vacuum level. $e\Phi_M$ is the work function and E_{FM} is Fermi level of the metal. E_V represents valence band and E_C represents conduction band of the semiconductor. E_{FS} is Fermi level, $e\Phi_S$ is work function of semiconductor. $e\chi$ is the electron affinity, which is the energy between the vacuum level and bottom of conduction band of semiconductor.

Figure 4.5 shows the energy levels when the metal and the semiconductor are in touch. Fermi level in a system must remain constant at thermodynamic equilibrium so when the junction is formed the Fermi levels should line up and remain flat in the

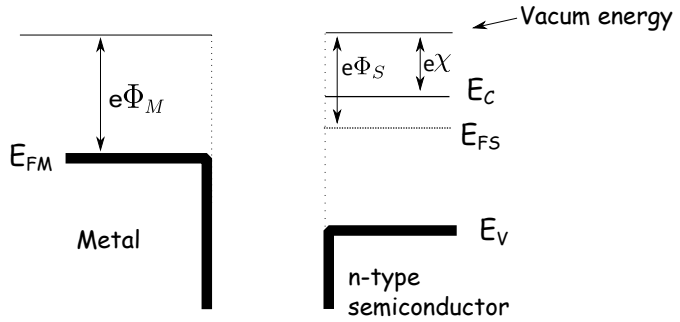

Figure 4.4. Various important energy levels in the metal and the semiconductors with respect to vacuum level [27].

absence of any externally applied potential difference. To ensure the continuity of the vacuum level and keep the Fermi level flat, Fermi level must move deeper into the band gap of semiconductor at interface region [27]. This results from the movement of electrons from semiconductor side to metal side. Because the metal side has big amount of electron density, movement of small amount of electrons does not affect the Fermi level or band profile of the metal. As electrons move to the metal side from the semiconductor side, they leave positively charged holes behind, so dipole region is formed similar to the one that is formed in the case of a p-n junction. An electric field is created and the field opposes the further drift of electrons so that equilibrium is formed and a depletion region with a width of W is created (See Figure 4.5).

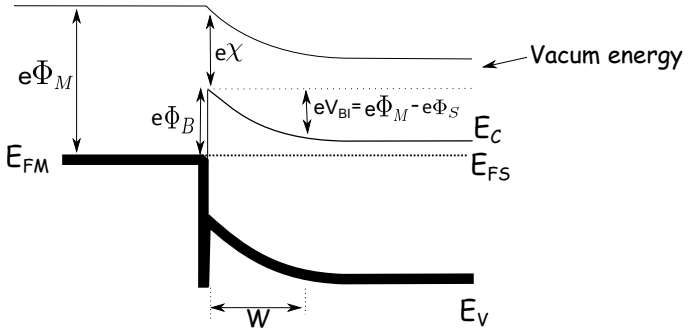

Figure 4.5. The junction potential when the metal and semiconductor brought together [27].

At the metal semiconductor junction, difference between the semiconductor conduction band and the metal Fermi level is defined as the height of the Schottky barrier (See Equation 4.1).

$$e\Phi_B = e\Phi_M - e\chi \tag{4.1}$$

While electrons move from semiconductor side to metal side they feel a potential barrier, eV_{BI} (See Figure 4.5), which is called built-in potential of the junction and is given by

$$eV_{BI} = e\Phi_M - e\Phi_S \tag{4.2}$$

Like in the case of p-n junction diodes, when an external potential difference is applied between two ends of the diode, the height of the potential barrier can be altered. Figure 4.6 shows the energy levels when a Schottky diode with n-type semiconductor is biased.

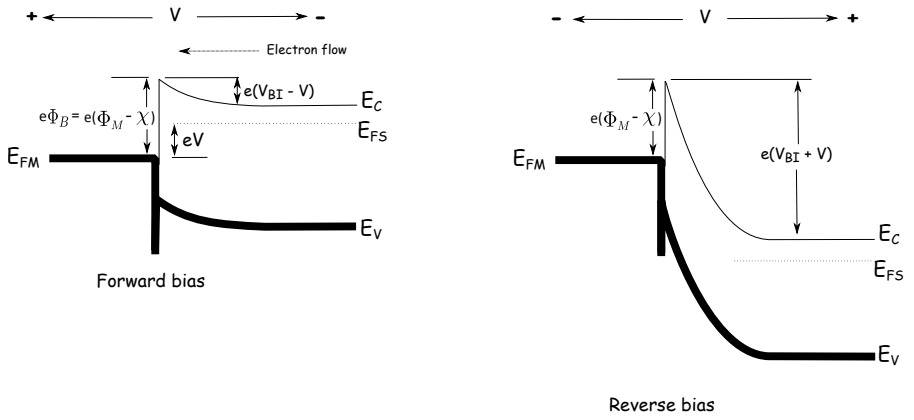

Figure 4.6. Forward and reverse biased Schottky diode [27].

On the left side of Figure 4.6, schematic of a Schottky diode which is forward biased with an external potential difference V, is shown. Electrons with energy greater than the barrier height, $e(V_{BI} - V)$, can overcome the barrier and pass across the junction. Forward bias allows the electrons flow from semiconductor side to metal side and create a current.

When a Schottky diode is reverse biased with a potential difference V, as in figure 4.6, the potential barrier height becomes $e(V_{BI} + V)$. There occurs an electric field which drags electrons from metal to semiconductor side, resulting in a leakage current. Compared to p-n junction diodes, Schottky diodes have greater reverse leakage current.

4.4. AC Equivalent Circuit of a Diode

An ideal diode can be considered as an element which allows current through it in one direction but not in the other. That is to say it acts like a short circuit while it was forward biased and acts like open circuit when it is reverse biased. However, when diodes are examined, it can be seen that the diode packages have some parasitics.

Voltage current characteristics of a p-n junction diode are given in Figure 4.3. When the slope of the graph for a voltage value is calculated, the dynamic resistance of the diode, R_D, for this voltage value can be obtained. In p-n junction, there also occurs a junction capacitance, C_j, resulting from separation of charges. Junction capacitance is very like an ordinary capacitor and can be determined by using the cross sectional area, A, of the junction, permittivity, ϵ, of used material and width, W, of the junction [27] (See Equation 4.3).

$$C_j = \frac{\epsilon A}{W} \tag{4.3}$$

The difference of junction capacitance from an ordinary capacitor is that the width of the junction changes as the voltage across the junction changes. During reverse bias the externally applied potential pulls charges apart so the width of the junction grows while during forward bias the charges are pushed close to each other resulting a smaller width and higher junction capacity.

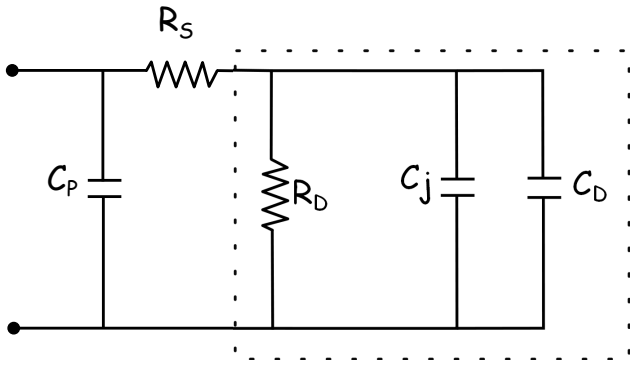

Figure 4.7. Forward biased equivalent circuit of a p-n junction diode [27].

During the forward bias of the diode, charges move through it. The amount of charge pass through the diode is related to the current. When the voltage across the diode changes to a different value, different amount of charge will be transmitted. This change in the amount of charges transmitted and change in the potential value cause a diffusion capacitance, C_D, which adds to junction capacitance. AC equivalent circuit for p-n junction diode in forward bias case is given in Figure 4.7 where R_D, C_j and C_D are parallel to each other. The resistance R_S is the series resistance of the neutral n-type and p-type semiconductor regions and the capacitance C_P is the capacitance associated with the diode packaging. For the reverse bias case of a p-n junction diode, the diffusion capacitance, C_D, vanishes.

Figure 4.8 represents the equivalent circuit of a Schottky diode. As in the case of p-n junction diode, there occurs the parallel combination of dynamic resistance, R_D, and junction capacitance, C_j. These two are in series with the resistance R_S, which includes the resistance of neutral semiconductor regions and contact resistance, and parasitic inductance, L_S. Finally, device geometry capacitance, C_{geom}, must also be included. If the device length is L, C_{geom} can be found as follows:

$$C_{geom} = \frac{\epsilon A}{L} \tag{4.4}$$

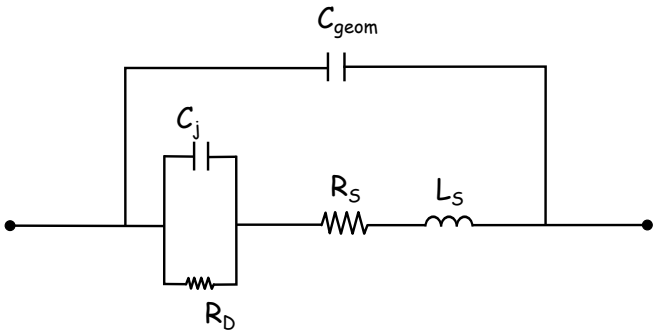

Figure 4.8. AC equivalent circuit of a Schottky diode [27].

4.5. Comparison of P-n Junction Diodes and Schottky Diodes

As seen from the equivalent circuits of p-n junction diodes and Schottky diodes (See Figures 4.7 and 4.8), being majority carrier devices, Schottky diodes do not have

diffusion capacitance which harms the performance of p-n junction diodes in the forward bias mode.

For p-n junction diode in forward bias case, current is carried by both majority and minority carriers. When the diode is in forward bias case and then the bias is removed, the diode continues to conduct because of minority carriers that are stored in p-n junction. The minority carriers need a certain time to recombine with opposite charges and to be neutralized. This time is called reverse recovery time of the diode [28]. Schottky diodes are majority charge carrier devices so they do not have reverse recovery time. Schottky diodes have faster response so that they are more suitable for high frequency operations.

When compared to p-n junction diodes, Schottky diodes have relatively low forward voltage drop. However, during reverse bias, leakage current for Schottky diodes are higher than p-n junction diodes.

5. HIGH FREQUENCY RECTIFICATION

A rectifier is an electrical device that converts alternating current to direct current and this process is called rectification. Rectifiers are the most important part of the RF recovery concept because the efficiency of the recovery system is mostly based on the efficiency of rectifying units. The most challenging task for rectifying unit is to design an efficient rectifier that operates at 200MHz and at high power levels.

Rectifier circuits employ diodes for allowing current flow through it in one direction but not in the other. As explained in Sections 4.2 and 4.3, diodes have leakage current when reverse biased and this current harms the operation of diode at high frequencies. Furthermore, in Section 4.4, real life diodes are explained and equivalent circuit of a diode is given. Parasitic parameters like junction capacity and lead inductance of diodes produce undesirable effects at high frequencies, so conventional rectifier circuits can not operate satisfactorily at the frequency of 200MHz. In order to have an efficient rectifying unit one must employ more novel circuit methods and considerable design efforts must be expanded in order to compensate the effects of these parasitic parameters.

In order to have an efficient rectifier one must choose a proper diode with low junction capacity and low lead inductance. However, because the parasitics of a diode and leakage current are inevitable, one must also employ a rectifying circuit which positively utilizes leakage current, lead inductance and junction capacitance of rectifier diodes as part of a resonant rectifier circuit [29].

In this chapter different types of resonant rectifier circuits will be given and simulation results for rectifier circuits will be compared.

5.1. Resonant Rectifier Circuits

5.1.1. Voltage Output Series Resonant Rectifier

Voltage output series resonant rectifier circuit is shown in Figure 5.1. The capacitor, C_j, that is in parallel with the diode, represents the junction capacitance.

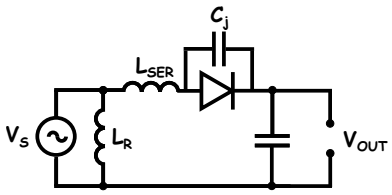

Figure 5.1. Voltage output series resonant rectifier.

In the circuit an inductance L_{SER} is placed in series with the diode. When the value of the inductance is chosen carefully, junction capacitance can resonate with it at the input frequency. L_{SER}, together with the C_j and lead inductance of diode, behaves as resonant circuit and the input current of negative cycle is stored at passive circuit elements and delivered to the output on the next positive cycle [5]. The shunt impedance, L_R at the input also resonates and it is needed to provide a path for the DC current [30].

5.1.2. Current Output Series Resonant Rectifier

Current output series resonant rectifier circuit employs two identical diodes (See Figure 5.2). Capacitors labeled as C_j represent junction capacitances. Including two diodes increases the power rating of the rectifier circuit and allows continuous current flow through the circuit.

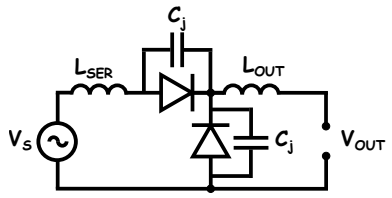

Figure 5.2. Current output series resonant rectifier.

The values of the inductances L_{SER} and L_{OUT} must be chosen so that they resonate with junction capacitances and lead inductances of diodes. The operation of this circuit will be explained in detail in Section 5.3.

5.1.3. Current Output Class E Resonant Rectifier

The circuit in Figure 5.3 is similar to the one in Section 5.1.2. The diode which is in series with L_{SER} is replaced by a capacitor. C_j again represents the junction capacity of the diode. This circuit is inverted version of a Class E rectifier [5]. Circuit analysis for a class E rectifier can be found in [31].

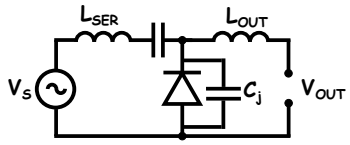

Figure 5.3. Current output class E resonant rectifier.

This circuit, having only one diode, has less power handling capacity when compared to the one in section 5.1.2. As in the case of previous circuit, carefully chosen circuit elements will result in a resonant operation and provide continuous current flow through the circuit.

5.1.4. Voltage Output Class F Resonant Rectifier

The circuit in Figure 5.4 consists of an input filter a rectifying diode, a transmission line as an output filter and a shunt capacitor at the output. Input filter should prevent harmonics to flow back to source [22]. Output filter prevents AC components to appear at load terminals. For more details about circuit operation see [22]. This circuit also employs only one diode so the power handling capacity is low.

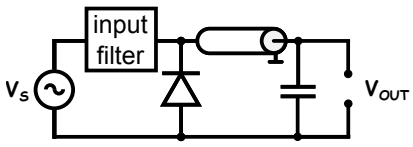

Figure 5.4. Voltage output class F resonant rectifier.

5.2. Simulations

Circuit simulations[2] were made with PSpice. SPICE (Simulation Program for Integrated Circuits Emphasis) is general purpose analog and mixed-mode circuit simulator for verifying circuit design and predict the circuit behavior. PSpice is a PC version of SPICE.

For simulations, diode GS150TC25110 which is developed by IXYSRF/Directed Energy, Inc. is used. Diode GS150TC25110 is a high power gallium arsenide Schottky diode with low package inductance for RF applications. Some properties of the diode can be seen in Table 5.1. PSpice model editor is used for modeling diode for simulations. In order to model a diode with PSpice model editor, diode characteristics must be read from the datasheet and a series of data points must be used for curve fitting with PSpice model editor. PSpice model editor requires data for forward current versus forward voltage, junction capacitance versus reverse bias voltage, leakage current versus reverse voltage and its reverse breakdown characteristics of the diode.

Table 5.1. Some properties of GS150TC25110 GaAs Schottky diode which is developed by IXYSRF/Directed Energy, Inc.

Property	Value
I_{Max}	10 A
V_{Max}	250 V
C_j	18pF (for reverse bias around 200 V)

Schematic of a circuit used for simulations can be seen in Figure 5.5. Source voltage, V_S, and source resistance, R_S, together represent the source. R_L is the load resistance for DC output. Frequency of V_S is 200MHz which is operational frequency of SPS.

Procedure for simulations can be summarized as follows [5]:

- The power delivered to rectifier circuit must be adjusted to operational area of

[2]Credits for simulations go to Michael Betz.

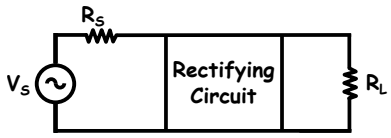

Figure 5.5. Schematic that is used for simulations.

interest. If the input impedance of rectifying circuit is equal to R_S the power delivered to circuit can be calculated from the Equation 5.1. Setting $V_S = 200$V and $R_S = 25\Omega$ will result a power level of 200W.

$$P_{DC} = \frac{V_S^2}{8R_S} \tag{5.1}$$

- Next step is to adjust R_L so that for the diodes used in rectifying circuit maximum current and voltage ratings are approached (See Table 5.1). R_L and V_S are varied and one cycle of the voltage across the diode and current through the diode is plotted. Optimum R_L value is the one which gives the closest voltage and current values to the maximum values of the diode.

- After determining the optimum R_L value the next step is to tune the rectifier components for resonant operation. In order to check that, input voltage and current of the rectifier can be plotted and phase voltage and current is compared. If there is no phase shift between voltage and current the input impedance of rectifying circuit is purely resistive.

- Next step is to match the source resistance to input impedance of the rectifier. This must be done without changing the power level which is delivered to the circuit because the input impedance of the rectifier changes with the input power level. Because it is not practical to change source resistance in real application, there will be an impedance matching network in RF/DC units (See Figure 3.3).

In order to check the efficiency and input impedance of the rectifier in different power levels, after the circuit is tuned, a parametric transient simulation can be run [5].

Simulation results for circuits in section 5.1 were plotted. Results are given in Figures 5.6 and 5.7. Figure 5.6 shows the efficiency over input power of rectifier and Figure 5.7 shows the magnitude of input impedance of the rectifier circuits over input power.

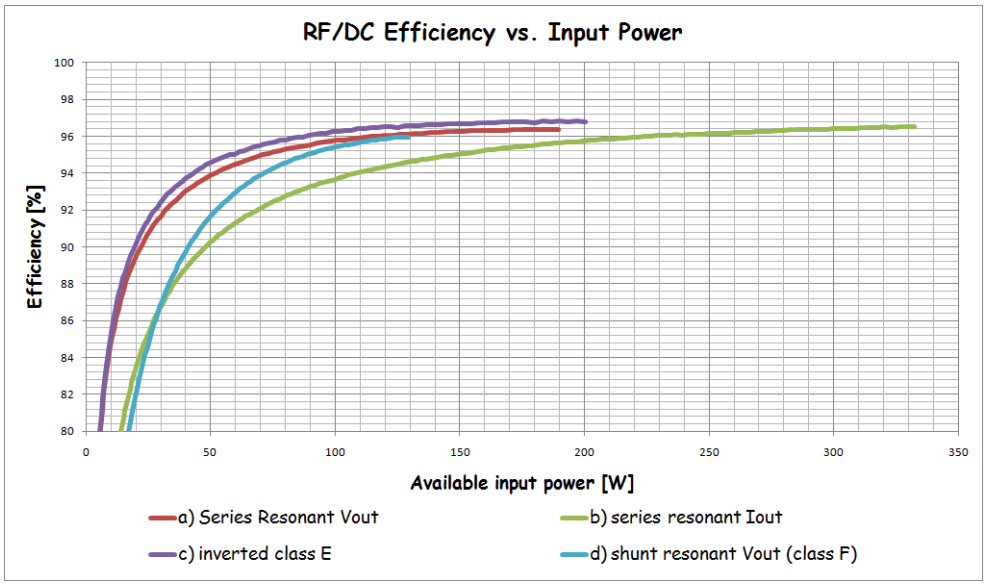

Figure 5.6. Efficiency of the rectifier circuits over different power levels.

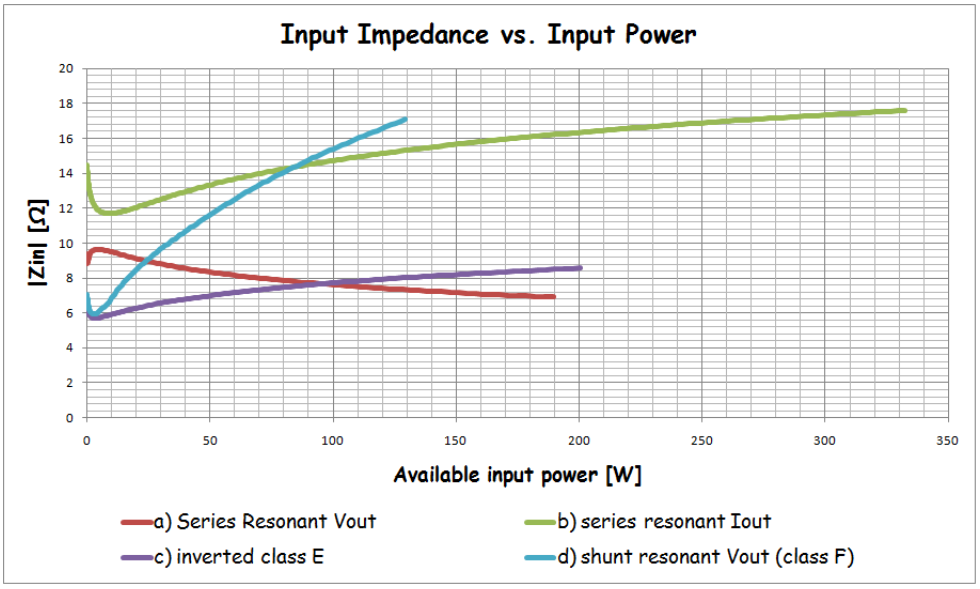

Figure 5.7. Magnitude of input impedances of rectifier circuits over different input power levels.

Current Output Series Resonant Rectifier (See Section 5.1.2), which is labeled as "b" in figures, was chosen as most suitable circuit. It has higher power handling capability than other circuits. The prototype of this circuit was produced and measurements were performed (See Chapter 6).

5.3. Current Output Series Resonant Rectifier

5.3.1. Operation of the Circuit

In Figure 5.8, the circuit components and the direction of the currents through them are shown. Diodes are labeled as D_1 and D_2. Because resonant rectifier circuit positively utilizes lead inductance and junction capacitance of the diodes as part of the circuits, the junction capacitances are also shown in figure. Lead inductances are not shown in the figure but it should be kept in mind that, together with L_{SER} they resonate with the junction capacitance.

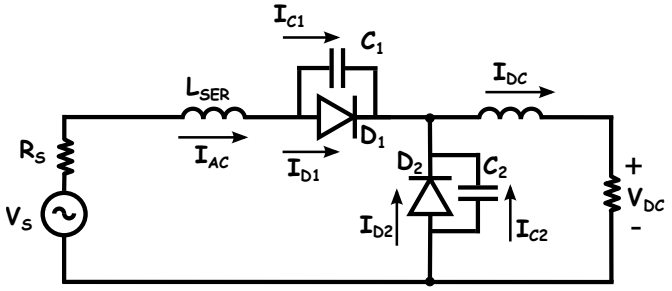

Figure 5.8. Circuit components and the direction of the current through them [32].

In Figure 5.9, current values through the circuit components and voltage values across the diodes during a complete cycle is given.

This circuit is basically a half-wave resonant rectifier and the operation of the circuit can be explained as follows:

- As seen in Figure 5.9, at time t_0 current through D_1 is equal to I_{AC} and I_{DC}. That is to say all the current reaching to load is passing through D_1 at time t_0 and no current passes through D_2.

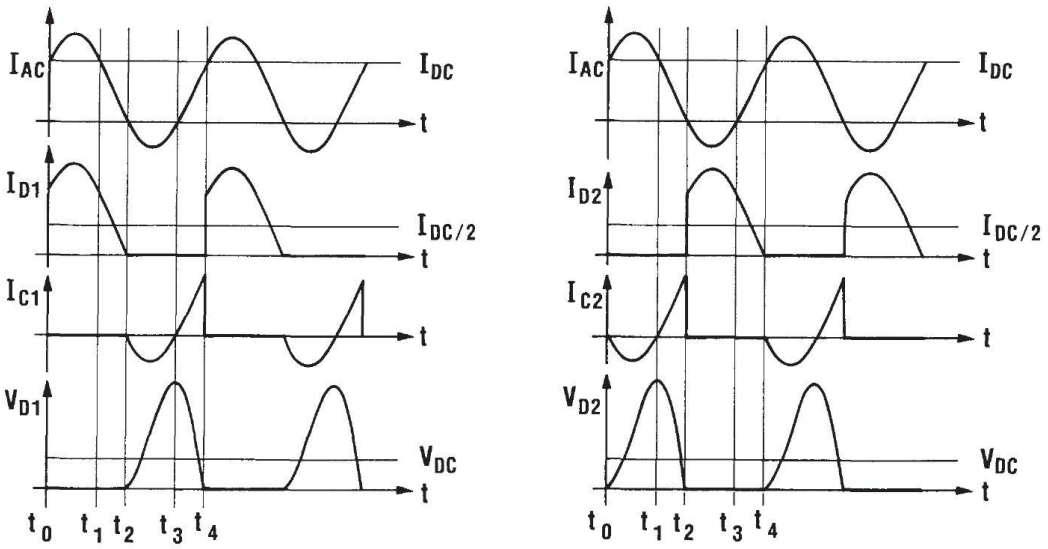

Figure 5.9. Current values through the circuit components and voltage values across the diodes during once complete cycle [32].

- After time t_0 value of I_{AC} is bigger than I_{DC}. Current passing through the D_1 is divided into who and the difference between I_{D1} and I_{DC} pass through the junction capacity of the second diode (See Figure 5.10). That way C_2 is charging between t_0 and t_1 and increases the voltage across the D_2. C_2 charges until time t_1 when the currents I_{AC} and I_{DC} are again equal. At time t_1 no current passes through C_2 and voltage across the D_2 is maximum.

- Between times t_1 and t_2 the value of I_{AC} smaller than I_{DC}. After time t_1, C_2 discharges and difference between I_{AC} and I_{DC} flows through C_2 (See Figure 5.10). As C_2 discharges voltage across D_2 decreases until time t_2 when the capacitance is completely discharged. At time t_2 when C_2 is completely discharged, D_2 becomes forward biased and current shifts from C_2 to D_2. The current shift is contained within the semiconductor so the total current through the diode is smooth. When I_{D1} and I_{C1} or I_{D2} and I_{C2} in Figure 5.9 are added it can be seen that the total currents through the diodes have a smooth waveform.
- Between times t_2 and t_3, diode D_1 is reverse biased. D_2 conducts and junction capacitance C_1 charges (See Figure 5.11). C_1 charges until t_3 when the voltage across D_1 is maximum.

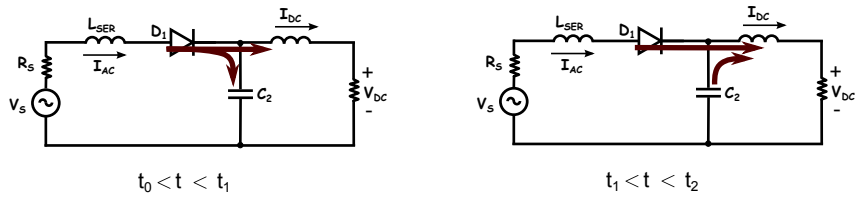

Figure 5.10. Flow of currents between times t_0 and t_2 when the first diode is forward biased.

- After time t_3, voltage across the first diode decreases and C_1 discharges so current I_{C1} adds to I_{D2} (See Figure 5.11). At time t_4 C_1 discharges completely and D_1 starts conducting and I_{AC} is again equal to I_{DC}.

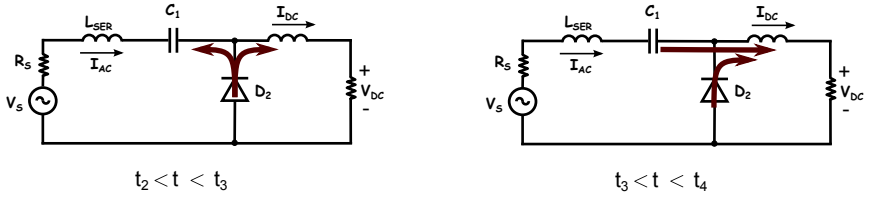

Figure 5.11. Flow of currents between times t_2 and t_4 when the second diode is forward biased.

5.3.2. PSpice Simulation

Circuit of current output series resonant rectifier that is used for PSpice simulations is shown in Figure 5.12. Diode GS150TC25110 which is developed by IXYSRF/Directed Energy, Inc. was modeled (See Section 5.2) and used for PSpice simulations. Diodes are labeled as D_1 and D_2 in the figure. In Figure 5.12, there are inductances L_P at both sides of each diode. L_P inductances represent package inductances of diodes and 1.5nH was chosen as the value of L_P [5].

In the figure, at the input of rectifier, there is an inductor L_{IF} and a capacitor C_{IF}. Choosing L_{IF}=19.19nH and C_{IF}=33pF will give us an LC circuit which resonate at the fundamental frequency of the circuit which is 200 MHz. This LC circuit acts like an input filter which attenuates higher order harmonics so that avoids reflection of harmonics to the source. It also provides a path for the DC current and avoids

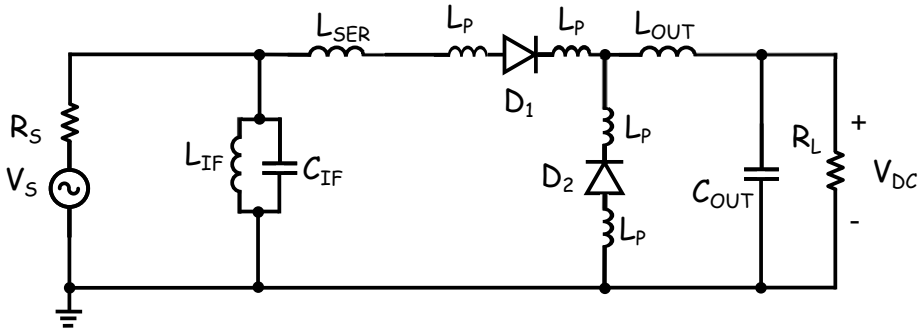

Figure 5.12. Circuit that is used for PSpice simulations.

any power dissipation at source resistance. RF circulator is to be used for RF/DC modules to avoid any reflected power back to RF cavity (See Section 3.2 and Figure 3.3). Circulators are designed so that they operate in a specific frequency band. The circulator must operate around 200MHz so there must not be reflected power back to input at higher frequencies.

At the output of rectifier, inductor L_{OUT} and capacitor C_{OUT} form an output filter. Choosing the high values for output inductor and output capacitor will allow only DC current to flow at the output. For PSpice simulations values are set to L_{OUT}=150nH and C_{OUT}=200pF [5].

Series inductor L_{SER} and DC load resistor R_L can be used to tune the rectifier (See Section 5.2. The DC output voltage, V_{DC}, is equal to average voltage across the diode D_2 [32]. Changing R_L value will change the value of V_{DC} so that the average voltage across the diode D_2. As reverse bias voltage across the diode rises, junction capacity of the diode decreases so changing R_L value will change the junction capacitance of the diode. Together with package inductances, L_P, series inductance, L_{SER}, resonates with junction capacitances. After setting the value of R_L to a value which gives the voltage across the diode close to the maximum value the value of L_{SER} can be set to a value where we have resonant operation. L_{SER} was set to 14nH for PSpice simulations [5].

When the prototype of the circuit is built, it is not practical to change the value of L_{SER}, so only way to tune the rectifier for different input power levels is to change

R_L. After setting L_{SER} to a value where we have resonant operation, R_L can be used to tune the circuit for different input power levels. As the input power level of the rectifier increases the current through the R_L will increase as well as V_{DC}. Increase in V_{DC} will result in an increase in the average voltage across the diode D_2 and decrease in junction junction capacity. Change in capacity will harm the resonant operation and so that R_L must be decreased to reach a lower voltage value across the diode.

6. CONSTRUCTION OF PROTOTYPE AND MEASUREMENTS

In this chapter, construction of a prototype of current output series resonant rectifier (See Section 5.3) will be explained and measurement methods and measurement results will be given.

6.1. Construction

Constructed circuit is the one in Figure 5.12. In order to avoid reflection and have maximum power transfer prototype has a matching network which is explained in Section 6.1.1.

Diode GS150TC25110 which is developed by IXYSRF/Directed Energy, Inc. was used for prototype. The diode package has three diodes inside. Two diodes were needed for the prototype so one was left unused. For the construction, wire wound inductors, SMD capacitors and a copper clad board were used. The traces on the clad board were cut by hand. As explained in Section 5.3.2 only way to tune the rectifier after construction is to change the value of R_L so an adjustable resistor was used.

The inductors were produced by wounding a magnet wire (copper wire which is covered by thin insulator). The shape was first estimated using a formula and several inductors were produced. The inductors were soldered to SMA connector and the values were tested using a calibrated VNA.

For the first measurements, a quarter wave impedance transformer was used (See Section 6.1.1.1). At one end, the transformer was soldered to circuit board and at the other end, in order to connect it to source, a 50Ω SMA connector was soldered to it (See Figure 6.1).

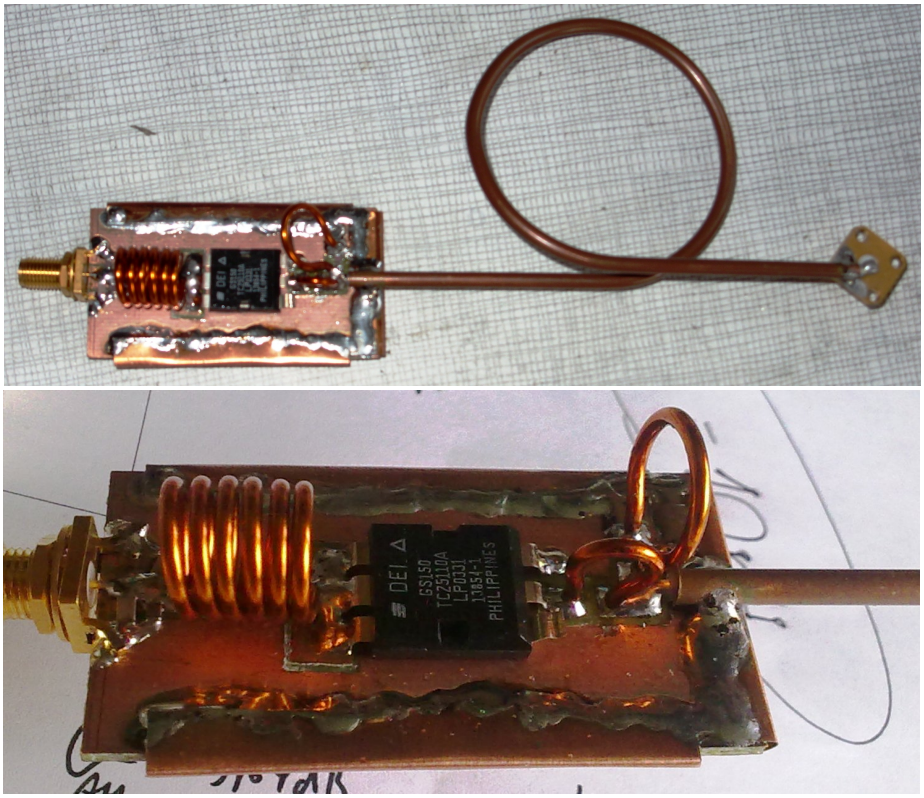

Figure 6.1. Prototype of current output series resonant rectifier circuit.

6.1.1. Impedance Matching

As mentioned in Section 5.2, matching of input impedance of the rectifier to source resistance was made manually during simulations. However it is not practical in real life. Excess power from RF cavity is carried away by coaxial cables with characteristic impedance of Z_0=50Ω. In order to have a matched circuit, so that maximum power transfer from coaxial lines to rectifier circuit, we need a matching unit between coaxial line and rectifier circuit. For matching unit two different methods were employed and measurements for rectifier circuit with both matching techniques were performed.

6.1.1.1. Quarter Wave Impedance Transformer. Quarter wave impedance transformer is actually a transmission line whose length is exactly one forth of the wave traveling inside it. Quarter wave impedance transformer can be used for transforming a purely resistive impedance value to another purely resistive value. In Figure 6.2 a coaxial transmission line whose characteristic impedance is Z_1 is placed between a load with impedance Z_L and coaxial line with characteristic impedance Z_0.

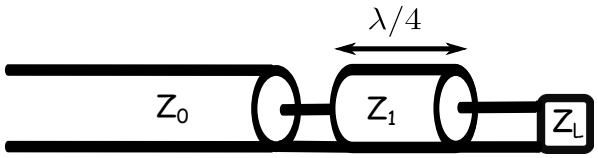

Figure 6.2. Schematic of matching with a quarter wave transformer.

Impedance, Z_{IN}, seen by the coaxial line with characteristic impedance Z_0 is given by the Equation 6.1 [33].

$$Z_{IN} = \frac{Z_1^2}{Z_L} \tag{6.1}$$

For maximum power transfer impedance seen by the coaxial line must be equal to its characteristic impedance. When Z_0 is equal to Z_{IN} all the energy that is carried by the coaxial line with characteristic impedance Z_0 is transferred to load without any reflection. Equating Z_0 to Z_{IN} and using Equation 6.1 give us the characteristic impedance of quarter wave impedance transformer as in Equation 6.2.

$$Z_1 = \sqrt{Z_0 Z_L} \tag{6.2}$$

For 200W input power the rectifier circuit has impedance around $Z = 16.4\Omega$ (See Figure 5.7). In order not to have a reflection this impedance must be matched to characteristic impedance (Z_0=50Ω) of coaxial lines which carry RF energy from power divider (See Figure 3.3). For matching quarter wave impedance transformer with characteristic impedance Z_1=28.63Ω is needed. Electrical length of quarter wave impedance transformer is $l_{el} = 0.37m$ for 200MHz frequency. However coaxial lines are produced with specific characteristic impedances and most common coaxial cable impedances are 50Ω, 75Ω. 25Ω coaxial cable was available at laboratory so for the first measurements a quarter wave impedance transformer which was produced of 25Ω coaxial cable was used.

Figure 6.3 shows, on the Smith chart, the transformation of the rectifier circuit $Z = 16.4\Omega$ at 200W using quarter wave impedance transformer with characteristic impedances Z_1=28.63Ω and 25Ω. While Z_1=28.63Ω transformer transforms the

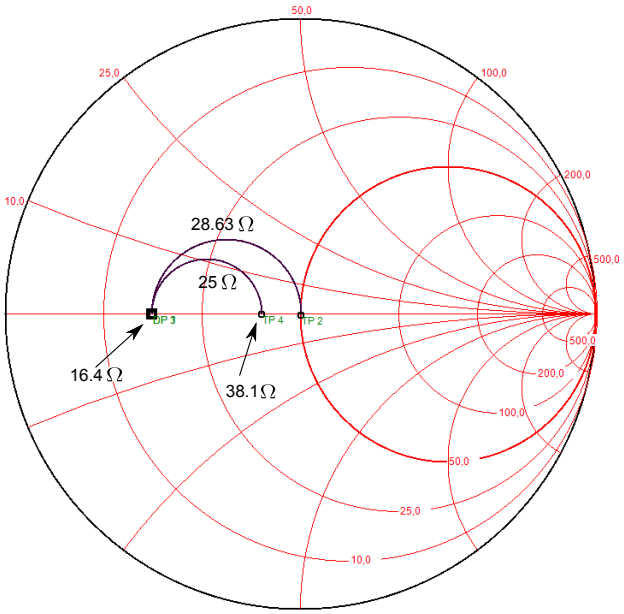

Figure 6.3. Representation of matching with a quarter wave impedance transformer on a Smith chart.

impedance to 50Ω, 25Ω transformer transforms it to 38.1Ω where we would have some amount of reflection. 25Ω transformer matches the the impedance of the rectifier best for $Z_L = 12.5\Omega$ which corresponds to a small input power level of rectifier.

Because the electrical length of the cable is not the same as real length, the real length must be found in order to use this transformer. The real length of the quarter wave impedance transformer was determined with vector network analyzer (VNA). First the quarter of the wave length of the EM wave inside the cable was estimated and the cable was cut into that length. Then the cable was connected to a properly calibrated VNA and clipped carefully until we see short circuit at the open end[3] .

6.1.1.2. Two Section Series Impedance Transformer . One disadvantage of quarter wave impedance transformer is that the impedance value of required coaxial line segment is not always easily realized. This problem can be solved by using two section series impedance transformer shown in Figure 6.4. This transformer employs two line segments of known impedances Z_1 and Z_2 with adjusted electrical lengths L_1 and L_2 to match an impedance Z_L to a main line of impedance Z_0.

[3]Quarter wave impedance transformer transforms open end to short end and vice versa.

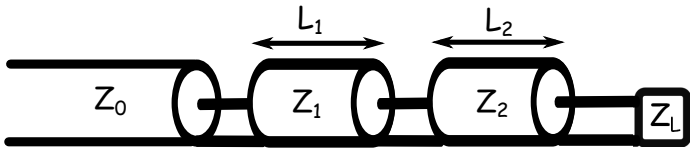

Figure 6.4. Schematic of matching with a two section series impedance transformer.

This transformer is more flexible about the choice of impedance values Z_1 and Z_2 because it is possible to employ different impedance values with different lengths for the same purpose (For more information about this transformer see [33]).

Because 50Ω and 25Ω coaxial lines were available at the laboratory, these impedance values were chosen. The required lengths were calculated using a MATLAB code taken from [33].

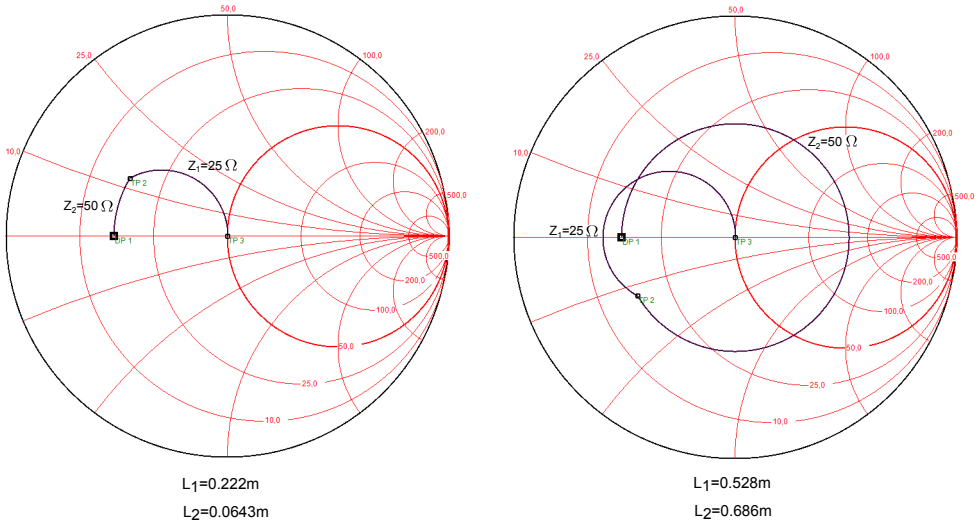

Figure 6.5. Representation two possible solutions of matching with a two section series impedance transformer on the Smith chart.

After running the code, MATLAB gives two solutions for given impedance values. For $Z_0 = 50\Omega$, $Z_1 = 25\Omega$, $Z_2 = 50\Omega$ and $Z_L = 16\Omega$ the first solution is $L_1 = 0.222m$ and $L_2 = 0.0643m$ and the second solution is $L_1 = 0.528m$ and $L_2 = 0.686m$. Figure 6.5 shows the representation of two possible solutions of matching with a two section series impedance transformer on the Smith chart.

While producing this transformer 25Ω coaxial section was adjusted to required length. Because the 50Ω section needed to be very short an SMA connector was used.

It was tested using a calibrated VNA and the matching was verified.

6.2. Measurements

In order to check the efficiency of the prototype, measurements were performed. Complex reflection coefficient was also found using the measurement data and analyzing data in MATLAB. In order to avoid any failure and keep the circuit safe, pulsed power was used during the measurements. Used pulse length for all measurements is 10μs and the pulse frequency is one second.

6.2.1. Measurement Setup

Setup that was used during the measurements is shown in Figure 6.6. VNA was used as RF signal source. It was set to operate in continuous wave mode at the frequency of 202.5MHz. Amplifier that was used was one of the old amplifiers which had been used for the operations of Linac2[4] . Amplifier operates at 202.5MHz and it is able to give power up to 400W. A trigger was connected to amplifier to arrange the operation time of the amplifier so that pulsed power with pulse length of 10μs and the pulse frequency of one second was obtained.

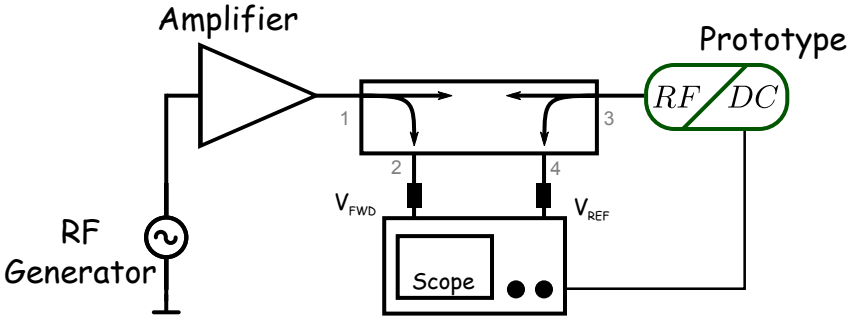

Figure 6.6. Schematic of the setup that was used for measurements of the prototype [5].

Between the prototype and the amplifier a four-way broadband directional coupler was used for measuring the amplifier output power, P_{AMP}, and reflected power from the prototype (See Figure 6.6). As it seems in the Figure 6.6 the first port was connected

[4]Linac2 is a linear accelerator at CERN's accelerator complex.

to amplifier, the second port was connected to an oscilloscope in order to measure P_{AMP}, the third port was connected to prototype and forth port was also connected to oscilloscope for measuring reflected power from the prototype. The output of rectifier was also connected to oscilloscope in order to measure the voltage across the load resistor at the output of the rectifier. In order to secure the oscilloscope additional attenuators were used between the oscilloscope and second and forth port of directional coupler. Attenuations were measured with VNA together with the directional coupler.

Even the pulse length was 10μs, the digital oscilloscope that was used for measurements was fast enough to see the actual waveform of the amplifier, output power and reflected power from the prototype as well as the DC output power. That allows us to see the phase shift between incident power on the rectifier and reflected power from the rectifier and calculate the complex reflection coefficient.

6.2.2. Measurement Methods

RF/DC conversion efficiency of the rectifier can be found from the ratio of DC output power of the rectifier and input power on rectifier which is P_{IN}. The attenuation between the first port of the directional coupler and prototype is small and can be ignored so P_{IN} can be taken equal to P_{AMP}. Second port of the directional coupler was connected to the oscilloscope to measure P_{AMP}. In order to calculate it from the value that is read from the oscilloscope we need to know the total attenuation between first port of directional coupler until it reaches the oscilloscope. Total attenuation results from the followings:

- Coupling of directional coupler between first and second port.
- Cables that were used for power transfer.
- Additional attenuators that were placed to protect the oscilloscope.

Overall attenuation factor G_{ATT} was measured with VNA. Taking into account that the oscilloscope has RF compatible inputs with a characteristic impedance of 50Ω,

P_{IN} can be calculated using Equation 6.3.

$$P_{IN} = \frac{V_{RMS}^2}{50} 10^{G_{ATT}/10} \tag{6.3}$$

In Equation 6.3, G_{ATT} is in decibel and V_{RMS} is the root mean square of the forward voltage value, V_{FWD}, measured at oscilloscope channel which is connected to second port of the directional coupler.

V_{RMS} value was calculated in MATLAB using equation 6.4.

$$V_{RMS} = \sqrt{\frac{1}{N} \sum_{n=1}^{N} V_{FWD}^2(n)} \tag{6.4}$$

In equation 6.4, n represents the data points. The oscilloscope was set to five giga-samples per second rate which gives 10^5 sample points in 20μs time window. For the calculations, only a slice, from 6μs to 7μs was used, where the circuit is in steady state [5]. Data points were saved and exported to computer and analyzed in MATLAB.

DC output voltage, V_{DC}, across the load of prototype can be used to calculate output DC power, P_{DC}, of rectifier using Equation 6.5.

$$P_{DC} = \frac{V_{DC}^2}{R_L} \tag{6.5}$$

Because the oscilloscope was fast enough to see the actual waveform of input and reflected power, we can calculate the reflection coefficient. Reflection coefficient is defined as the ratio of reflected and incident wave at the input of the rectifier. Complex reflection coefficient Γ can be calculated using Equation 6.6 where $\hat{V}_{REF}$ and $\hat{V}_{FWD}$ are the amplitude of reflected and forward voltage values read from the oscilloscope and, ϕ_{REF} and ϕ_{FWD} are phase angles of the reflected and forward voltages relative to a

fixed point (See [5] for more information).

$$\Gamma = \frac{\hat{V}_{REF}e^{i\phi_{REF}}}{\hat{V}_{FWD}e^{i\phi_{FWD}}} \tag{6.6}$$

6.2.3. Measurement Results

A series of measurements were performed for the constructed prototype sweeping different power levels. Two different types of measurements performed using quarter wave impedance transformer. During the first one R_L left constant. It was set to a value in order to have least reflection around P_{IN}=200W. During the second measurement with quarter wave impedance transformer R_L was optimized so that we had least reflection at each power level. Efficiency values of both measurements are given in Figure 6.7.

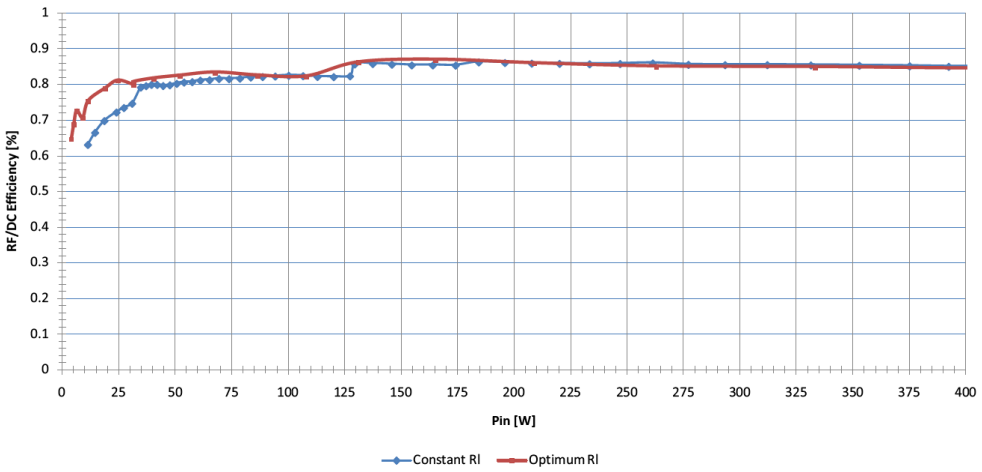

Figure 6.7. Efficiency of prototype with quarter wave impedance transformer for different power levels.

As seen from the Figure 6.7, both with constant R_L and optimized R_L the efficiency is higher than 80 per cent for the input power levels higher than 50W. The efficiency goes up to 85 per cent around 150W input power.

Figure 6.8 shows the complex reflection coefficients on the Smith chart. On the left, the reflection coefficients from the measurements with constant R_L are shown.

On the right, the reflection coefficients from the measurements with optimized R_L are shown. While for constant R_L, there is no power level where the rectifier input impedance is matched to coaxial line characteristic impedance, for the optimized R_L rectifier is matched quite good for the power levels around 35W. In Section 6.1.1.1, it was shown that the quarter wave impedance transformer should match the circuit for impedance value of 12.5Ω which corresponds a power level around 35W in simulations (See Figure 5.7).

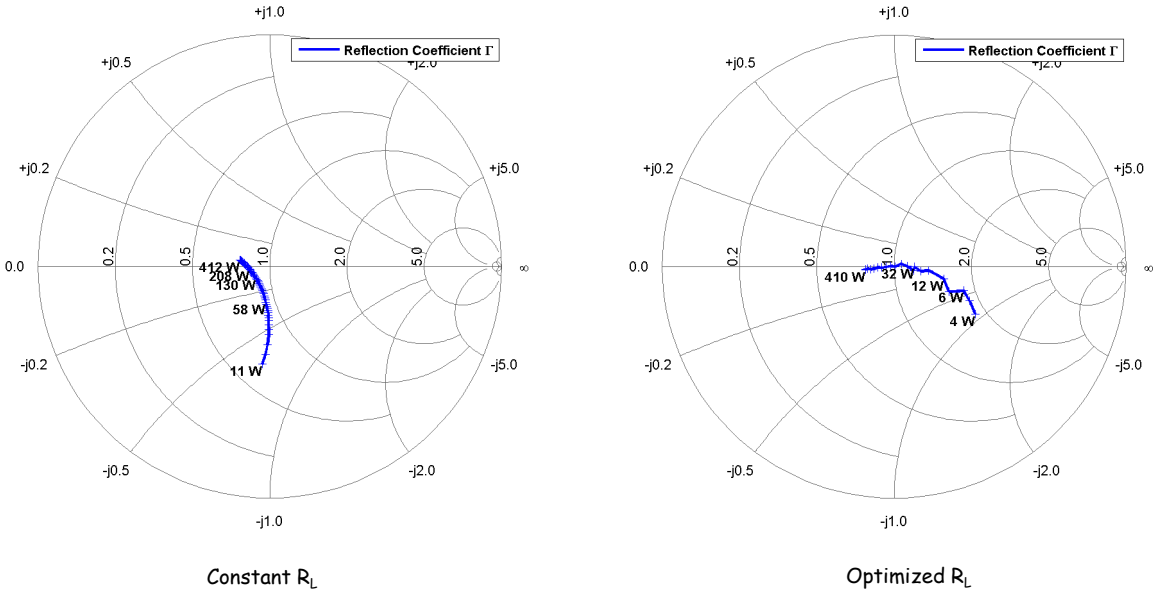

Figure 6.8. Reflection coefficients of rectifier with quarter wave impedance transformer for different power levels.

After measurements with quarter wave impedance transformer, the transformer was replaced by two section series impedance transformer. The SMA connector which was used for 50Ω section (See Section 6.1.1.2) of transformer was soldered to circuit board. The measurement results with the two section series impedance transformer is given in Figure 6.9. The efficiency approaches to 90 per cent at high power levels and, as expected, the rectifier is matched quite good at high power levels.

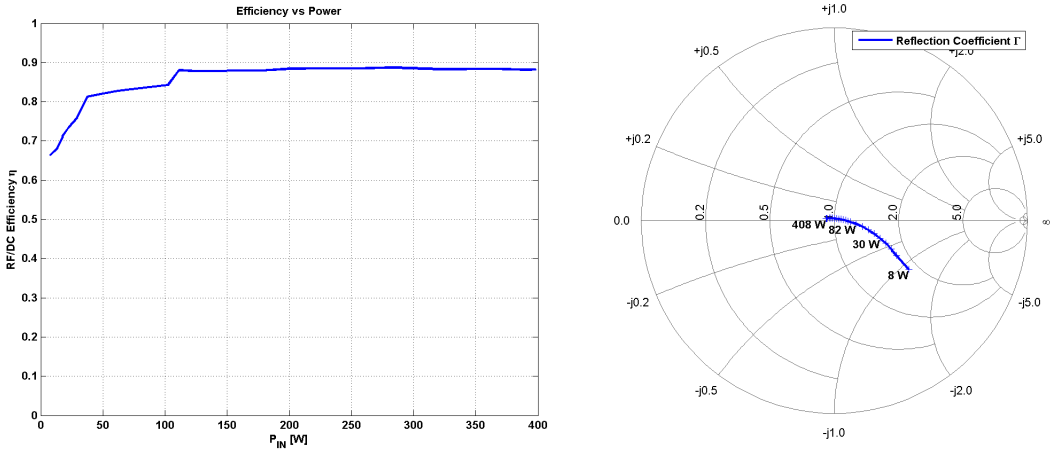

Figure 6.9. Efficiency and reflection coefficients of the prototype with two section series impedance transformer.

7. CONCLUSIONS

Not all the energy that is incident to RF cavities are transferred to particles. In fact, depending on the accelerating structure, big amounts of power is dissipated in load resistors. In Chapter 1, CERN's SPS accelerator was analyzed as an example and the importance of having efficient accelerators for ADS was mentioned.

In Chapter 2, possible ways of recovering the wasted power were explained and feasibility was discussed.

During the next chapters of this thesis the overall RF recovery system for SPS accelerating cavities was discussed. It was concluded that the RF/DC conversion is the most suitable choice for SPS frequency which is 200MHz. For RF/DC conversion resonant rectifier circuits which employ semiconductor diodes were chosen. PSpice simulation results showed that it is possible to convert RF power at frequency 200MHz into DC power with efficiencies higher than 90 per cent. Prototype of a selected resonant rectifier architecture was constructed with GaAs Schottky diodes. The biggest advantages of Schottky diodes over p-n junction diodes are low junction capacity and not having reverse recovery time.

Measurement results showed that it is possible to convert the RF power into DC power with an efficiency up to 88 per cent at 200MHz frequency. The efficiency and the power rating of the rectifiers can increase with the development of semiconductor technology. Measurements also showed that it is feasible to convert the RF power to DC power after SPS accelerating cavities instead of wasting it in load resistors.

REFERENCES

1. Bryant, P. J., and K. Johnsen, *The Principles of Circular Accelerators and Storage Rings*, Cambridge University Press, Cambridge, 1993.

2. L'Annunziata, M. F., *Radioactivity: Introduction and History*, Elsevier B. V., Amsterdam, 2007.

3. Chao, A. W., H. O. Moser, and Z. Zhao, *Accelerator Physcs, Technology and Applications*, World Scientific Publishing, River Edge, 2004.

4. Lee, S. Y., *Acelerator Physics*, second edition, World Scientific Publishing, Singapore, 2004.

5. Betz, M., *Feasibility Study for High Power RF Energy Recovery in Particle Accelerators*, M.S. Thesis, Hochshule Karlsruhe Technik und Wirtschaft, 2010.

6. CERN Document Server, *SPS accelerating cavity*, 2008, http://cdsweb.cern.ch/record/969105, 2010.

7. Boussard, D., G. Dôme, and T. P. R. Linnecar, "Acceleration in the CERN SPS Present Status and Future Developements", 8^{th} *Particle Accelerator Conference*, San Francisco, 1979, CERN, Prévessin, 1979.

8. Dôme, G., "The SPS Acceleration System Traveling Wave Drift-Tube Structure for the CERN SPS", *Proton Linear Accelerator Conference*, Chalk River, Ontario, Canada, 1976, CERN, Geneva, 1977.

9. Kapoor, S. S., "Accelerator-Driven Sub-Critical Reactor System (ADS) for Nuclear Energy Generation", *Pramana-Journal of Physics*, Vol. 59, No. 6, pp. 941-950, 2002.

10. Zamani, M., M. Fragopoulou, M. Manolopouluo, S. Stoulos, R. Brandt, W. Westmeier, M. Krivopustov, A. Sosnin, and S. Golovatyuk, "Experience Gained During

10 Years Transmutation Experiments in Dubna", *Journal of Physics*, Conference Series 41, pp. 475-483, 2006.

11. Singh, P., S. V. L. S. Rao, R. Pande, T. Basak, S. Roy, M. Aslam, P. Jain, S. C. L. Srivastava, R. Kumar, P. K. Nema, S. Kailas, and V. C. Sahni. "Accelerator Developement in India for ADS Programme", *Pramana-Jourlan of Physics*, Vol. 68, No.2, pp. 331-342, 2007.

12. Wiedemann, H., *Particle Accelerator Physics*, third edition, Springer Berlin Heidelberg, New York, 2007.

13. Boltezar, E., H. Haseroth, W. Pirkl, G. Plass, T. R. Sherwood, U. Tallgren, P. Têstu, D. Warner, and M. Weiss, "PERFORNAMCE OF THE NEW CERN 50MeV LINAC", *IEEE Transactions on Nuclear Science*, Vol. NS-26, No. 3, 1979.

14. Gerigk, F., and M. Vretenar, "LINAC4 Technical Design Report", CERN, Geneva, 2006.

15. Gerigk, F., "Conceptual Design of the SPL II", CERN, Geneva, 2006.

16. Butterworth, A., M. E. Angoletta, L. Arnaudon, P. Baudrenghien, J. Ferreira Bento, T. Bohl, O. Brunner, E. Ciapala, F. Dubouchet, G. Hagmann, W. Höfle, T. Linnecar, P. Maesen, J. Molendijk, E. Montesinos, J. Noirjean, A. Pashnin, V. Rossi, J. Sanchez-Quesada, M. Schokker, E. Shaposhnikova, D. Stellfeld, J. Tuckmantel, D. Valuch, U. Wehrle, F. Weierud, and R. Sorokoletov, "FIRST BEAM COMMISSIONING OF THE 400 MHz LHC RF SYSTEM", *Proceedings of PAC09*, Vancouver, British Columbia, Canada, 2009.

17. Matsumoto, H., V. A. Vanke, and N. Shinohara, "Microwave/DC Cyclotron Wave Converter Having Decreased Magnetic Field", United States Patent, No: US 6,507,152 B2, 2003.

18. Vanke, V., *High Power Converter of Microwaves into DC*, 1999,

http://jre.cplire.ru/iso/sep99/1/text.html, 2010.

19. Brown, W. C., "The History of Power Transmission by Radio Waves", *IEEE Transactions on Microwave Theory and Techniques*, Vol. MTT-32, No.9, 1984.

20. Brown, W. C., "The Technology and Application of Free-Space Power Transmission by Microwave Beam", *Proceedings of the IEEE*, Vol.62, No. 1, 1974.

21. Caspers, F., M. Betz, A. Grudiev, and H. Sapotta, "Design Concepts for RF-DC Conversion in Particle Accelerator Systems", *Proceedings of IPAC10*, Kyoto, Japan, 2010.

22. Gutmann, R. J., and J. M. Borrego, "Power Combining in an Array of Microwave Power Rectifiers", *IEEE Transactions Microwave Theory and Techniques*, Vol. MTT-27, No. 12, 1979.

23. Hamrouni, N., and A. Chérif, "Modelling and Control of a Grid Connected Photovoltaic System", *Revue des Energies Renouvelables*, Vol. 10 N.3, pp. 335-344, 2007.

24. Azab, M., "A New Maximum Power Point Tracking for Photovoltaic Systems", *Proceedings of World Academy of Science, Engineering and Tehcnology*, Volume.34, 2008.

25. Orozco, M. I. A., J. R. Vázquez, P. Salmerón, S. P. Litrán, and F. J. Alcántara, "Maximum Power Point Tracker of a Photovoltaic System Using Sliding Mode Control", *International Conference on Renewable Energies and Power Quality (ICREPQ09)*, Valencia, Spain, 2009.

26. Nelkon, M., *Principles of Atomic Physics & Electronics*, Heinemann Educational Books, London, 1976.

27. Singh, J., *Semiconductor Devices: Basic Principles*, John Wiley & Sons, Inc., New York, 2001.

28. Rashid, M. H., *Power Electronics: Circuits, Devices, and Applications*, Pearson Educational Inc., New Jersey, 2004.

29. Bowman, W. C., F. M. Magalhaes, W. B. Suiter, and N. G. Ziesse, "Resonant Rectifier Circuit", United States Patent, Patent Number: 4,685,041, 1987.

30. Rivas, J., *Radio Frequency dc-dc Power Conversion*, Ph.D. Thesis, Massachusetts Institute of Technology, 2006.

31. Kazimierczuk, M. K., B. Tomescu, and A. Ivaşcu, "Class E Resonant Rectifier with a Series Capacitor", *IEEE Transactions on Circuits and Systems*, Vol.41, No.12, 1994.

32. Nitz, W. A., W. C. Bowman, F. T. Dickens, F. M. Magalhaes, W. Strauss, W. B. Suiter, and N. G. Ziesse, "A New Family of Resonant Rectifier Circuits for High Frequency DC-DC Converter Applications", *IEEE Applied Power Electronics Conference and Exposition*, 1988,

33. Orfanidis, S. J., *Electromagnetic Waves and Antennas*, 2008, http://www.ece.rutgers.edu/∼orfanidi/ewa, 2010.